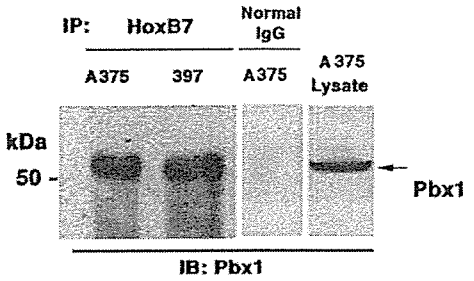

Figure 5 Pbx1 binds HoxB7. Interaction between Pbx1 and HoxB7 as assessed by immunoprecipitation. A375 and 397 cell lysates were immunoprecipitated with anti-HoxB7 antibody and immunoblotted with anti-Pbx1 antibody. Sodium dodecyl sulfate–polyacrylamide gel electrophoresis was carried out under the non-reducing condition.

of Pbx1 with the siRNAs slightly reduced the mRNA expression of HoxB7 (Figure 6a). It remains uncertain whether Pbx1 binds directly to the promoter region of the HoxB7 gene. HoxB7 is reported to regulate the expression of basic fibroblast growth factor (bFGF), angiopoietin-2 (Ang-2), matrix metalloprotease 9 (MMP9), growth-related oncogene-α (GROα), interleukin-8 (IL-8) and vascular endothelial growth factor (VEGF) (Care *et al.*, 1996, 2001). We thus evaluated the effects of Pbx1 knockdown on the expression of the target genes. As shown in Figure 6b, knockdown of Pbx1 markedly reduced the level of bFGF mRNA, and mildly did those of Ang-2 and MMP mRNAs, whereas those of GROα, IL-8 and VEGF were unchanged. Pbx1 knockdown significantly reduced protein levels of Ang-2 and MMP9, but it did not seem to have any effect on the protein levels of bFGF. This may be owing to the short culture duration and/or long half-life of bFGF protein. We obtained similar results in 397 cells (data not shown).

We further examined whether enforced expression of PLZF in melanoma cells would reduce HoxB7, bFGF, Ang-2 and MMP9. Quantitative RT–PCR analysis revealed that transcripts of all of these were significantly reduced in both A375P and 397P cells (Figure 7). These data suggest that the PLZF–Pbx1 axis is important in regulating HoxB7 target genes via Pbx1/HoxB7 heterocomplex formation.

Discussion

In this study, we performed DNA microarray analysis and found that Pbx1 is a prominent transcription factor targeted by PLZF. Pbx1 was highly expressed in the A375 and 397 cell lines, and its expression was markedly reduced by the expression of PLZF. Moreover, we showed that the growth suppression caused by ectopic expression of PLZF is reversed by enforced expression of Pbx1. Knockdown of Pbx1 using siRNAs in A375 and 397 cells reduced its protein levels by approximately 80%. Pbx1 siRNAs significantly inhibited cell growth in culture, thus suggesting that Pbx1 is a downstream target of PLZF in melanoma cell growth regulation.

In order to determine whether PLZF suppresses Pbx1 gene expression directly or indirectly, we examined the ability of PLZF to repress the Pbx1 promoter. We found that the 3.0 kb upstream region of the Pbx1 gene (nucleotides −3.0 kb to 0) contains seven possible PLZF DNA-binding consensus sequences. We then performed reporter assay and EMSA to examine the direct binding of PLZF in the Pbx1 promoter region. EMSA suggested the presence of an interactive site (Site 1) for PLZF in the 3.0-kb of upstream Pbx1 gene sequences. Deletion of Site 1, however, did not recover Pbx1 gene expression. These data suggest multiple direct and/or indirect regulation mechanisms for Pbx1 gene expression by PLZF. Further analysis is required for elucidating these mechanisms.

Pbx1 was originally identified at t(1;19) chromosomal translocations in acute pre-B-cell leukemias (Kamps *et al.*, 1990; Nourse *et al.*, 1990), and it has also been described as a transcriptional activator. Pbx1 is known to interact with a number of Hox proteins through the YPWM motif located at the N-termini of the homeodomains in Hox proteins and to regulate the function of Hox proteins (Chang *et al.*, 1995; Shanmugam *et al.*, 1997). It has been reported that Pbx1 cooperates in the cellular proliferation and transformation induced by Hox proteins (Krosl *et al.*, 1998). Krosl *et al.* (1998) showed that the ability of HoxB4 and HoxB3 to interact with Pbx1 is critical for transformation of Rat-1 cells, that Hox proteins have a notable effect on cell growth, and that Pbx1 further enhances this effect. Although HoxB7 is reportedly involved in melanoma growth (Care *et al.*, 1996, 2001; Felicetti *et al.*, 2004), there have been few reports on the relationship between Pbx1 and the progression of melanoma. We showed here that immunoprecipitation of HoxB7 from A375 and 397 melanoma cell lines co-precipitated a 52-kDa protein that was recognized by an anti-Pbx1 antibody, thus suggesting that Pbx1 physically interacts with HoxB7. Our data indicate that Pbx1 plays an important role in melanoma growth and that it forms heterocomplexes with HoxB7, which suggests that molecular events mediated by the Pbx1–HoxB7 heterocomplex are altered in melanoma cells when Pbx1 is suppressed by PLZF.

Previous studies have identified some HoxB7 target genes. bFGF was identified as the main target of HoxB7 in melanoma cell lines (Care *et al.*, 1996). In addition, VEGF, GROα, IL-8, Ang-2 and MMP9 were found to be upregulated in HoxB7-transduced cells (Care *et al.*, 2001). Based on these reports, we analysed the effect of Pbx1 knockdown on HoxB7 target genes. We found that knockdown of Pbx1 slightly downregulated HoxB7 itself and substantially downregulated bFGF, Ang-2 and MMP9, but not VEGF, GROα or IL-8. This suggests that HoxB7 target genes are differentially regulated by HoxB7–Pbx1 or by another HoxB7 complex. Interestingly, these factors are strongly associated with tumor angiogenesis and invasion (Becker *et al.*, 1989; Ahmad *et al.*, 2001; Etoh *et al.*, 2001; Johnson *et al.*, 2004). The Pbx1–HoxB7 complex may

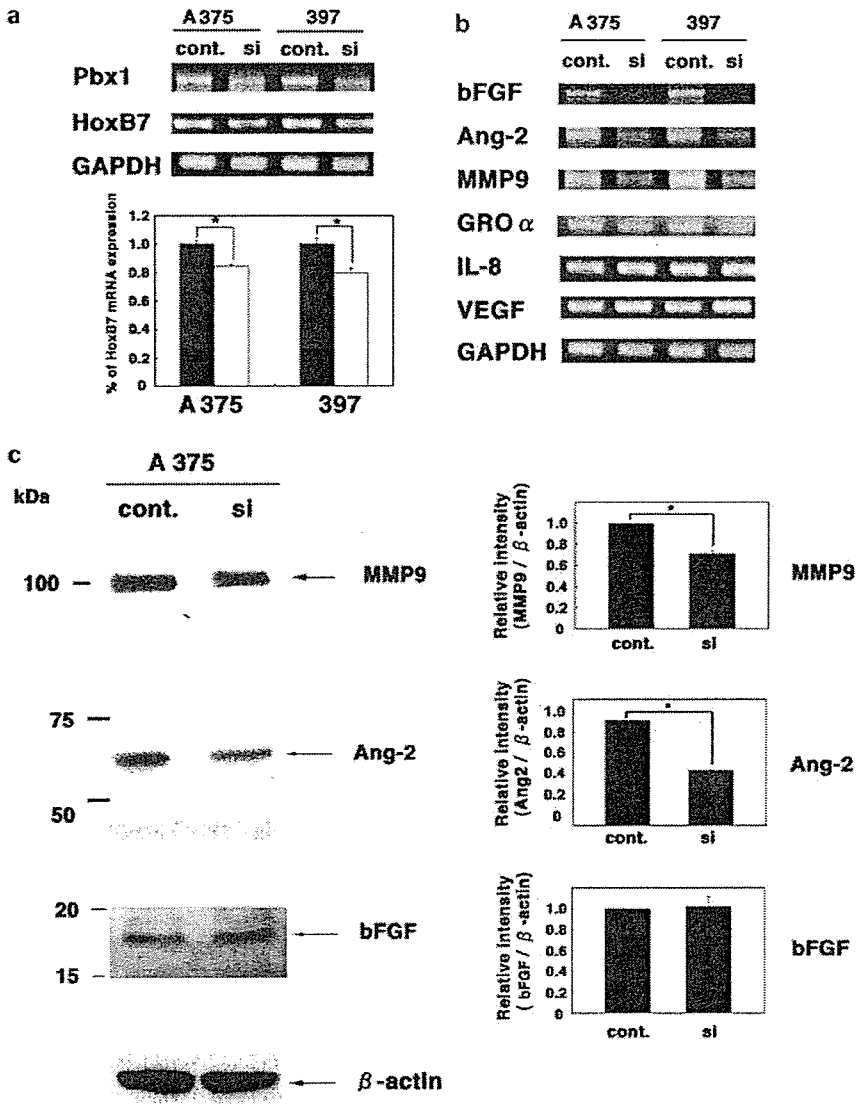

Figure 6 Expression of HoxB7 and its target genes is modulated by knockdown of Pbx1. (**a**) Upper panel: RT–PCR analysis of HoxB7 expression in Pbx1-knockdown melanoma cells and control cells. Lower panel: Relative intensity of Pbx1 and HoxB7 mRNA expression in Pbx1-knockdown melanoma cells and control cells, which was calculated as a ratio vs the expression of GAPDH. $^*P<0.05$. (**b**) RT–PCR analysis of HoxB7 target gene expression in each cell type. (**c**) Immunoblot analysis of Ang-2, MMP9 and bFGF in Pbx1-knockdown melanoma cells and control cells. Relative intensity of each protein was calculated as a ratio vs the expression of β-actin. $^*P<0.05$.

thus play a very important role in melanoma growth, and its suppression could be a major cause of the reduction in PLZF-mediated growth in melanoma. This is supported by previous reports that PLZF is expressed in melanocytes but not in melanoma cells, and that the pattern of PLZF expression inversely correlates with that of HoxB7 (Care *et al*., 1996, 1998).

In this study, we showed that the suppression of Pbx1 expression by PLZF downregulates some HoxB7 target genes, including bFGF, Ang-2 and MMP9. The data indicated that the changes in the molecular network caused by the loss of PLZF may play an important role in the progression of melanoma. Further analyses of the PLZF–Pbx1 network will assist in the discovery of target molecules for the development of novel anti-melanoma drugs.

Materials and methods

Materials

Human melanoma cell lines A375 and 397 were generously provided by Dr Kawakami (Keio University, Tokyo, Japan) (Sumimoto *et al*., 2004). Cells were grown in Roswell Park Memorial Institute medium 1640 supplemented with 10% fetal calf serum (FCS), penicillin (100 U/ml) and streptomycin

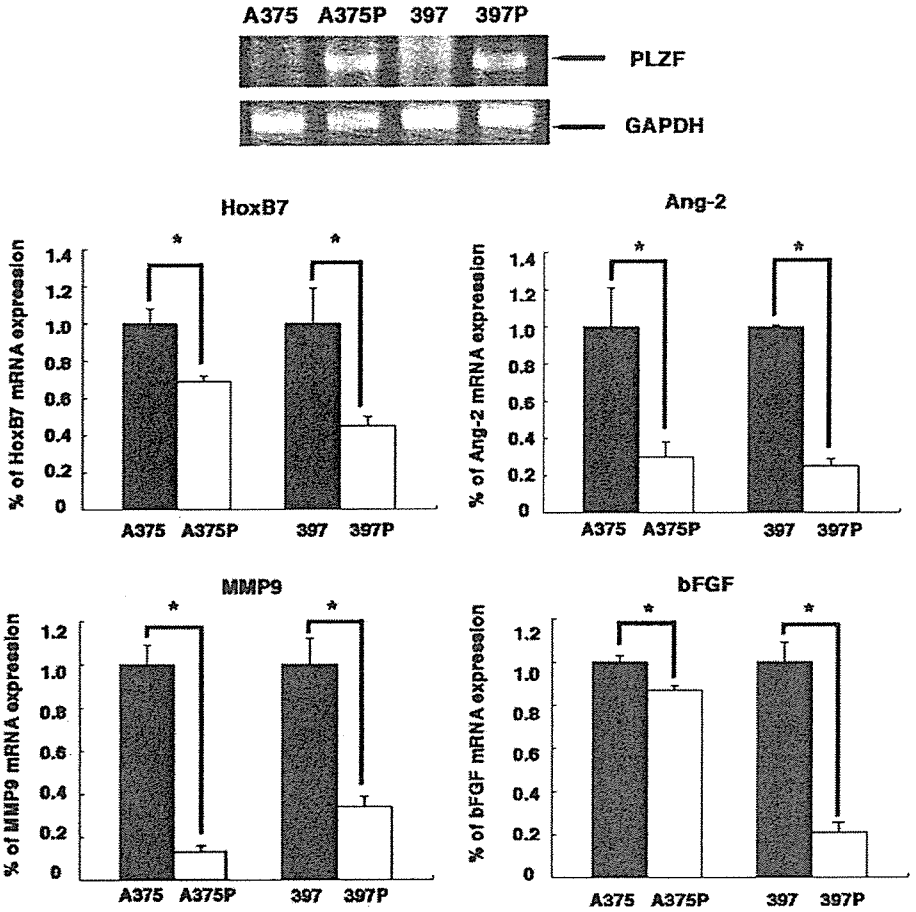

Figure 7 Expression of HoxB7, bFGF, Ang-2 and MMP9 is suppressed by the transduction of PLZF in melanoma cells. Upper panel: RT–PCR analysis for PLZF mRNA in A375, A375P, 397 and 397P cells. GAPDH, glyceraldehyde 3-phosphate dehydrogenase. PLZF was evaluated at 35 cycles, whereas control GAPDH evaluated at 24 cycles. Lower panel: qRT–PCR for HoxB7, bFGF, Ang-2 and MMP9 mRNA in PLZF-expressing melanoma cells and parental cells. $*P<0.05$.

sulfate (100 μg/ml) at 37°C in an atmosphere containing 5% CO_2. Antibodies used were as follows: rabbit anti-Pbx1 polyclonal antibody (Santa Cruz Biotechnology, Santa Cruz, CA, USA), mouse anti-PLZF monoclonal antibody (Oncogene Research Products, San Diego, CA, USA), rabbit anti-HoxB7 polyclonal antibody (CeMines, Golden, CO, USA), rabbit anti-bFGF polyclonal antibody (Abcam, Cambridge, UK), mouse anti-Ang-2 monoclonal antibody, goat anti-MMP9 monoclonal antibody (R&D, Tokyo, Japan), goat horseradish peroxidase-conjugated anti-rabbit antibody, donkey horseradish peroxidase-conjugated anti-goat antibody and goat horseradish peroxidase-conjugated anti-mouse antibody (Promega, Madison, WI, USA).

Plasmid and adenovirus vector construction

A plasmid encoding PLZF was generated by subcloning the human PLZF cDNA into pcDNA3.1/Hygro. (Invitrogen, Carlsbad, CA, USA). A plasmid encoding Pbx1 was generated by subcloning Pbx1 cDNA into pME18S (Tanaka *et al*., 2004). The Pbx1 promoter 3.0 kb was subcloned into pGL3 (Promega). Transfection of plasmids was performed with LipofectAMINE (Invitrogen) according to the manufacturer's instructions. To assess transfection efficiency of pME18S-Pbx1 in 375P cells, both PME18S-Pbx1 and pME18S-ECFP plasmids were transfected into 375P cells and CFP-positive cells were counted. Adenovirus vector (Ax) carrying PLZF was prepared using an adenovirus expression vector kit (Takara Biomedicals, Kyoto, Japan). PLZF was subcloned into the cosmid cassette pAxCAw. Ax containing the CA promoter and PLZF (AxPLZF) was generated by the COS-TPC method according to the manufacturer's protocol. A375 and 397 cells were infected with Axs at an MOI of 50–200 for 1 h. Ax expressing LacZ (Ax-LacZ) and GFP (Ax-GFP) were used as controls to exclude the effects of Ax itself.

RT–PCR and quantitative real-time PCR

Primer sequences for RT–PCR are listed in Table 2. Total RNA was isolated from cultured melanoma cells using Trizol Reagent (Invitrogen), and was treated with DNase I (Clontech, Palo Alto, CA, USA) at 37°C for 30 min to remove contaminating genomic DNA. RT–PCR was performed using RT–PCR High Plus (Toyobo, Osaka, Japan) according to the manufacturer's instructions. cDNA was reverse transcribed from total RNA for 30 min at 60°C, and heated to 94°C for 2 min. Amplification was performed using a GeneAmp PCR System 9700 (Applied Biosystems, Foster City, CA, USA) for

Table 2 Primer sequences used in this study

Gene	*Upper primer (5′–3′)*	*Lower primer (5′–3′)*
Pbx1	GGAGATTGAGCGGATGGT	CATGGGCTGACACATTGGTAG
HoxB7	AAGGAGCAGAGGGACTCGGACT	AAATCTTGATCTGTCTTTCCGTGAG
bFGF	CCCAAGCGGCTGTAC	ATACTGCCCAGTTCGTTTCA
Ang-2	GCAGCCTATAACAACTTTCGGAAGA	TATTTCTATCATCACAGCCGTCT
MMP9	GAGATGCGTGGAGAGTCGAAA	CAAAGGCGTCGTCAATCA
GROα	ACTGCTGCTCCTGCTCCTGGTAGCC	TTTCCGCCCATTCTTGAGTGT
IL-8	GAATCTAAATTATCAGTCATA	CAGTGAACATTATAGATCTAT
VEGF	CTGCTGTCTTGGGTGCATTG	TCACCGCCTCGGCTTGTCACA
GAPDH	CGTATTGGGCGCCTGGTCACCAG	TCGCTCCTGGAAGATGGTGATGGG

Abbreviations: Ang-2, angiopoietin-2; bFGF, basic fibroblast growth factor; GAPDH, glyceraldehyde-3-phosphate dehydrogenase; GROα, growth-related oncogene-α; IL-8, interleukin-8; MMP9, matrix metalloprotease 9; Pbx1, pre-B-cell leukemia transcription factor 1; VEGF, vascular endothelial growth factor.

24 or 35 cycles. The cycle profile consisted of 1 min at 94°C for denaturation and 1.5 min at 60°C for annealing and primer extension. To evaluate amplification, 5 μl of the reaction mixture was electrophoresed on a 1.0% agarose gel containing ethidium bromide. We performed at least three independent studies and confirmed similar results. Quantitative real-time PCR (qRT–PCR) was performed using the ABI PRISM 7700 sequencer detection system (Perkin–Elmer Applied Biosystems, Foster City, CA, USA). Primers and probe were purchased from Applied Biosystems (Assays-on-Demand). RT–PCR mixtures were prepared according to the manufacturer's instructions for the TaqMan One-Step RT–PCR Master Mix Reagent kit (Perkin–Elmer Applied Biosystems). Probe was labeled with a reporter fluorescent dye (6-carboxyfluorescein) at the 5′ end. For glyceraldehyde 3-phosphate dehydrogenase (GAPDH) detection, Pre-Developed TaqMan Assay Reagent (Perkin–Elmer Applied Biosystems) was added. The thermal conditions were 48°C for 30 min for RT and 95°C for 10 min, followed by 45 amplification cycles of 95°C for 15 s for denaturing and 60°C for 1 min for annealing and extension. PCR products were sequenced to confirm proper amplification. To compare mRNA expression, results were determined as relative values against GAPDH as an internal reference. There were $n=3$ samples in each group.

siRNA experiments

siRNA sequences used in this study were as follows: Pbx1 siRNA sequences were 5′-CCGCAGGGCATCAGTGCTA-3′ (siRNA1) and 5′-CGACAGAAATCCTGAATGA-3′ (siRNA2), and the mutated Pbx1 siRNA sequences were 5′-CC ACAAGGCATTAGCGCTA-3′ (mut. siRNA1) and 5′-CG ACCGAGATCCTAAACGA-3′ (mut. siRNA2) (B-Bridge International, Sunnyvale, CA, USA). Scrambled siRNA directed against 5′-GCGCGCTTTGTAGGATTCG-3′ was also used as a negative control. This sequence was not present in any mammalian mRNAs in the National Center for Biotechnology Information database. siRNA transfection was performed with CodeBreaker siRNA Transfection Reagent (Promega). Briefly, cells (5×10^5) were incubated in 35-mm plates with siRNA (final concentration, 40 nM)–CodeBreaker Reagent (15 μl) mixture in serum-free medium for 24 h. Cells were then grown in media with 10% FCS.

Microarray analysis

Total RNA was isolated from LacZ or PLZF Ax-infected melanoma cells at 48 h post-infection. The Acegene Human oligo chip 30K (Hitachi Software Engineering, Yokohama, Japan) containing 30 000 genes was used to compare gene expression in melanoma cells infected with PLZF or LacZ adenovirus. Arrays were screened according to the manufacturer's protocol. Fluorescent images of hybridized microarrays were obtained with a CRBIO IIe microarray scanner (Hitachi Software Engineering), and images were analysed with DNAsis Array software (Hitachi Software Engineering).

EMSA

Nuclear protein extracts were prepared using cellLytic NuCLEAR Extraction Kit (Sigma, St Louis, MO, USA). Biotin-labeled oligomers containing PLZF-binding sequences (Sites 1, 2, 3, 4, 5, 6 and 7) were bound to nuclear extracts. Binding reactions were performed using the LightShift EMSA Optimization and Control kit (Pierce, Rockford, IL, USA) according to the manufacturer's instructions. Reaction mixtures were incubated on ice for 60 min. Biotin-unlabeled oligomers were used as competitors, and when present, were added to the mixtures 30 min before the other reagents. Binding reactions were subjected to EMSA on 4% non-denaturing polyacrylamide gels in 0.5 × Tris-Borate-EDTA buffer, and detection was performed using a LightShift Chemiluminescent EMSA Kit (Pierce) according to the manufacturer's instructions. Sequences of the probes used in this study were as follows: Site 1, 5′-CCTCCAGATCCAGTT CATCC-3′; Site 2, 5′-CGGGGTAAGACAGTTGCAAT-3′; Site 3, 5′-TTTGAGTATATAGTTTTGTG-3′; Site 4, 5′-TTTAAAAAAACAGTTTAAAA-3′; Site 5, 5′-ACTGTG TACACAGTCAGATT-3′; Site 6 5′-AAAAATGACACA GTTTGGTA-3′; Site 7, 5′-GCTGGAACTACAGTAC CATT-3′ and mutated-Site 1, 5′-CCTCCAGAGAAAGTT CATCC-3′.

Luciferase reporter assays

Melanoma cells were cultured in 24-well plates and grown to 70% confluence. Cells were transfected with 0.8 μg/well of pGL3-Pbx1 plasmid DNA using LipofectAMINE (Invitrogen). Transfected cells were harvested at 24 h post-transfection, and lysates were assayed for luciferase activity with a Dual-Glo Luciferase Assay System (Promega) according to the manufacturer's protocol.

Immunoprecipitation and Western blotting

A375 and 397 cells were transiently transfected with pME18S-Pbx1 plasmid. Cells were lysed 48 h after transfection and equivalent amounts of lysate protein were subjected into immunoprecipitation. Immunoprecipitation and Western blotting were performed as described previously (Goishi *et al*.,

1995). After membranes were washed three times at intervals of 10 min with 0.05% Tween-20 in phosphate-buffered saline, horseradish peroxidase conjugate was detected by chemiluminescence with an ECL kit (Amersham, Buckinghamshire, UK) and autofluorography.

Acknowledgements

We thank Drs T Tsuda, T Jyokou, E Tan, M Tohyama, H Iwabuki, T Kikugawa, Y Kinugasa and E Koya for technical assistance, helpful comments and discussion.

References

Ahmad SA, Liu W, Jung YD, Fan F, Wilson M, Reinmuth N *et al.* (2001). The effects of angiopoietin-1 and -2 on tumor growth and angiogenesis in human colon cancer. *Cancer Res* **61**: 1255–1259.

Barna M, Hawe N, Niswander L, Pandolfi PP. (2000). Plzf regulates limb and axial skeletal patterning. *Nat Genet* **25**: 166–172.

Barna M, Merghoub T, Costoya JA, Ruggero D, Branford M, Bergia A *et al.* (2002). Plzf mediates transcriptional repression of HoxD gene expression through chromatin remodeling. *Dev cell* **3**: 499–510.

Becker D, Meier CB, Herlyn M. (1989). Proliferation of human malignant melanomas is inhibited by antisense oligodeoxynucleotides targeted against basic fibroblast growth factor. *EMBO J* **8**: 3685–3691.

Care A, Silvani A, Meccia E, Mattia G, Stoppacciaro A, Parmiani G *et al.* (1996). HOXB7 constitutively activates basic fibroblast growth factor in melanomas. *Mol Cell Biol* **16**: 4842–4851.

Care A, Silvani A, Meccia E, Mattia G, Peschle C, Colombo MP. (1998). Transduction of the SkBr3 breast carcinoma cell line with the HOXB7 gene induces bFGF expression, increases cell proliferation and reduces growth factor dependence. *Oncogene* **16**: 3285–3289.

Care A, Felicetti F, Meccia E, Bottero L, Parenza M, Stoppacciaro A *et al.* (2001). HOXB7: a key factor for tumor-associated angiogenic switch. *Cancer Res* **61**: 6532–6539.

Chang CP, Shen WF, Rozenfeld S, Lawrence HJ, Largman C, Cleary ML. (1995). Pbx proteins display hexapeptide-dependent cooperative DNA binding with a subset of Hox proteins. *Genes Dev* **9**: 663–674.

Chen Z, Brand NJ, Chen A, Chen SJ, Tong JH, Wang ZY *et al.* (1993). Fusion between a novel Kruppel-like zinc finger gene and the retinoic acid receptor-alpha locus due to a variant t(11;17) translocation associated with acute promyelocytic leukaemia. *EMBO J* **12**: 1161–1167.

Costoya JA, Hobbs RM, Barna M, Cattoretti G, Manova K, Sukhwani M *et al.* (2004). Essential role of Plzf in maintenance of spermatogonial stem cells. *Nat Genet* **36**: 653–659.

Etoh T, Inoue H, Tanaka S, Barnard GF, Kitano S, Mori M. (2001). Angiopoietin-2 is related to tumor angiogenesis in gastric carcinoma: possible *in vivo* regulation via induction of proteases. *Cancer Res* **61**: 2145–2153.

Felicetti F, Bottero L, Felli N, Mattia G, Labbaye C, Alvino E *et al.* (2004). Role of PLZF in melanoma progression. *Oncogene* **23**: 4567–4576.

Goishi K, Higashiyama S, Klagsbrun M, Nakano N, Umata T, Ishikawa M *et al.* (1995). Phorbol ester induces the rapid processing of cell surface heparin-binding EGF-like growth factor: conversion from juxtacrine to paracrine growth factor activity. *Mol Biol Cell* **6**: 967–980.

Heinemeyer T, Wingender E, Reuter I, Hermjakob H, Kel AE, Kel OV *et al.* (1998). Databases on transcriptional regulation: TRANSFAC, TRRD and COMPEL. *Nucleic Acids Res* **26**: 364–370.

Hong SH, David G, Wong CW, Dejean A, Privalsky ML. (1997). SMRT corepressor interacts with PLZF and with the PML-retinoic acid receptor alpha (RARalpha) and PLZF-RARalpha oncoproteins associated with acute promyelocytic leukemia. *Proc Natl Acad Sci USA* **94**: 9028–9033.

Johnson C, Sung HJ, Lessner SM, Fini ME, Galis ZS. (2004). Matrix metalloproteinase-9 is required for adequate angiogenic revascularization of ischemic tissues: potential role in capillary branching. *Circ Res* **94**: 262–268.

Kamps MP, Murre C, Sun XH, Baltimore D. (1990). A new homeobox gene contributes the DNA binding domain of the t(1;19) translocation protein in pre-B ALL. *Cell* **60**: 547–555.

Krosl J, Baban S, Krosl G, Rozenfeld S, Largman C, Sauvageau G. (1998). Cellular proliferation and transformation induced by HOXB4 and HOXB3 proteins involves cooperation with PBX1. *Oncogene* **16**: 3403–3412.

Li JY, English MA, Ball HJ, Yeyati PL, Waxman S, Licht JD. (1997). Sequence-specific DNA binding and transcriptional regulation by the promyelocytic leukemia zinc finger protein. *J Biol Chem* **272**: 22447–22455.

Mann RS, Chan SK. (1996). Extra specificity from extradenticle: the partnership between HOX and PBX/EXD homeodomain proteins. *Trends Genet* **12**: 258–262.

McConnell MJ, Chevallier N, Berkofsky-Fessler W, Giltnane JM, Malani RB, Staudt LM *et al.* (2003). Growth suppression by acute promyelocytic leukemia-associated protein PLZF is mediated by repression of c-*myc* expression. *Mol Cell Biol* **23**: 9375–9388.

Nourse J, Mellentin JD, Galili N, Wilkinson J, Stanbridge E, Smith SD *et al.* (1990). Chromosomal translocation t(1;19) results in synthesis of a homeobox fusion mRNA that codes for a potential chimeric transcription factor. *Cell* **60**: 535–546.

Shanmugam K, Featherstone MS, Saragovi HU. (1997). Residues flanking the HOX YPWM motif contribute to cooperative interactions with PBX. *J Biol Chem* **272**: 19081–19087.

Sumimoto H, Miyagishi M, Miyoshi H, Yamagata S, Shimizu A, Taira K *et al.* (2004). Inhibition of growth and invasive ability of melanoma by inactivation of mutated BRAF with lentivirus-mediated RNA interference. *Oncogene* **23**: 6031–6039.

Tanaka M, Nanba D, Mori S, Shiba F, Ishiguro H, Yoshino K *et al.* (2004). ADAM binding protein Eve-1 is required for ectodomain shedding of epidermal growth factor receptor ligands. *J Biol Chem* **279**: 41950–41959.

Wong CW, Privalsky ML. (1998). Components of the SMRT corepressor complex exhibit distinctive interactions with the POZ domain oncoproteins PLZF, PLZF-RARalpha, and BCL-6. *J Biol Chem* **273**: 27695–27702.

Yeyati PL, Shaknovich R, Boterashvili S, Li J, Ball HJ, Waxman S *et al.* (1999). Leukemia translocation protein PLZF inhibits cell growth and expression of cyclin A. *Oncogene* **18**: 925–934.

Journal of Dermatological Science (2007) 45, 69–72

ELSEVIER

Journal of Dermatological SCIENCE

www.intl.elsevierhealth.com/journals/jods

LETTER TO THE EDITOR

Epiregulin, a member of the EGF family, is over-expressed in psoriatic epidermis

KEYWORDS
Epiregulin; EGF family; Psoriasis; TGF-α; Amphiregulin; Northern blot; *In situ* hybridization

Psoriasis is characterized by the hyperproliferation of keratinocytes, altered epidermal differentiation, dermal angiogenesis, and a dense lesional infiltrate in the dermal and epidermal component, consisting mainly of macrophages, lymphocytes, and neutrophils. To date, the expression of many regulatory molecules has been well clarified in psoriatic epidermis. Previous reports have shown that various cytokines and growth factors are over-expressed in psoriatic epidermis [1]. Keratinocytes are the main component cells of the epidermis, and their growth is regulated by both positive and negative mediators [2]. Of these mediators, the most important mechanism for the proliferation of keratinocytes is the signal from the epidermal growth factor (EGF) receptor. The EGF family consists of EGF, transforming growth factor-α (TGF-α), heparin binding EGF-like growth factor (HB-EGF), amphiregulin, epiregulin, betacellulin, epigen, neuregulin (NRG)-1, NRG-2, NRG-3, and NRG-4, and the EGF receptor (EGFR) family consists of EGFR (also called ErbB1), ErbB2, ErbB3, and ErbB4 [2]. Previous reports have shown that TGF-α, amphiregulin and HB-EGF are over-expressed in psoriatic epidermis [3–5]. Given that epiregulin is a member of the EGF family and an autocrine growth factor for normal human keratinocytes [6], we speculated that epiregulin is over-expressed in psoriasis. To prove our hypothesis, we investigated the expression of epiregulin as well as TGF-α and amphiregulin in psoriatic epidermis.

All procedures that involved human subjects received prior approval from the Ethics Committee of Ehime University School of Medicine, Toon, Ehime, Japan, and all subjects provided written informed consent. Twelve psoriatic lesional skin samples and 10 normal healthy skin samples were obtained. To exclude the RNA from the dermis, we separated the epidermis from the dermis by a heat-separation technique. The specimens were heated at 60 °C in sterile saline for 1 min. The epidermis was then separated from the dermis, immediately frozen in liquid nitrogen. We confirmed that heat-separation did not influence on the results. Total RNA was extracted from snap-frozen epidermis by using Isogen (Nippon Gene, Tokyo, Japan). Northern blot analysis was performed as previously described [6]. TGF-α mRNA was detected in all the psoriatic

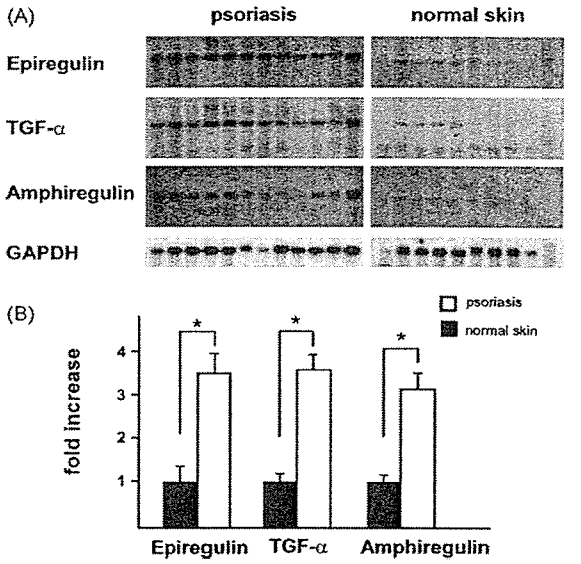

Fig. 1 mRNA expression of epiregulin, TGF-α, and amphiregulin in psoriatic epidermis. (A) The mRNA expression levels of epiregulin, TGF-α, and amphiregulin were analyzed by Northern blotting in psoriatic and normal epidermis. (B) Densitometric analysis of Northern blotting. Quantification of the signals was performed by using a densitometer and analyzed by ImageQuant software. Normal epidermis signal values were taken as 100% control. The signals were adjusted by GAPDH as an internal standard. $^{*}p < 0.05$.

doi:10.1016/j.jdermsci.2006.08.010

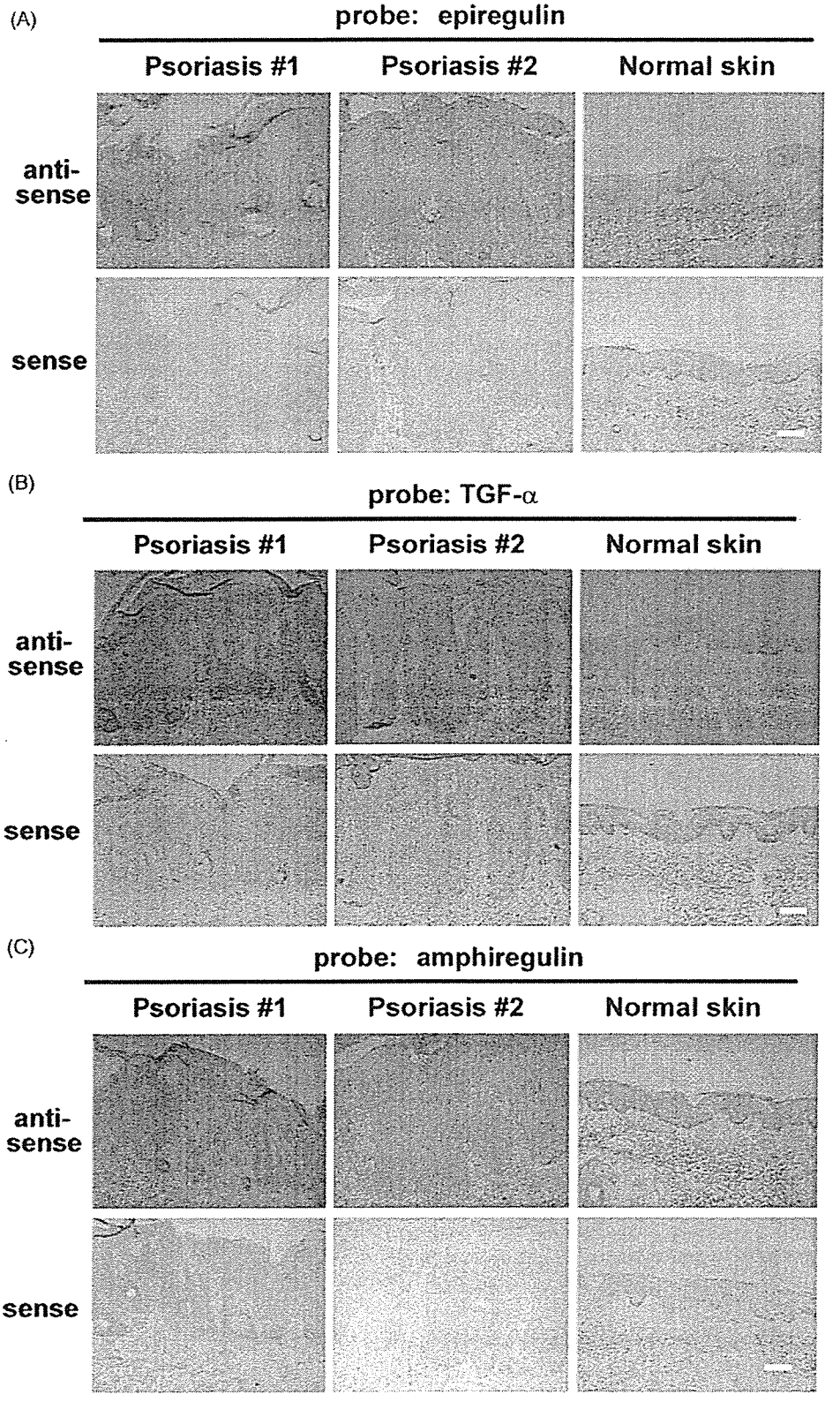

Fig. 2 *In situ* hybridization of epiregulin, TGF-α, and amphiregulin in psoriatic epidermis. *In situ* hybridization was performed using an automated *in situ* hybridization protocol. (A) Epiregulin; (B) TGF-α; (C) amphiregulin. Bar: 100 μm.

epidermis samples and was expressed at higher levels than in the normal epidermis. Amphiregulin mRNA was also detected in all the psoriatic epidermis samples and was expressed at higher levels than in the normal epidermis. The 4.8-kb transcript of epiregulin was detected in both normal and psoriatic epidermis, although the expression level was higher in the psoriatic epidermis than in the normal epidermis (Fig. 1A). Densitometric analysis revealed that TGF-α and amphiregulin mRNA were elevated by 3.6- and 3.2-fold, respectively. Epiregulin mRNA was also increased in psoriatic epidermis by 3.5-fold (Fig. 1B). To identify the localization of epiregulin, TGF-α, and amphiregulin mRNA, we performed *in situ* hybridization as previously described [7]. In normal skin, we found that epiregulin mRNA was expressed in the basal layer and that its expression was very faint. However, epiregulin mRNA was over-expressed in the spinous layer, mainly in the uppermost region of the spinous layer, but not in the basal layer of the psoriatic lesional epidermis (Fig. 2A). TGF-α and amphiregulin mRNA were also over-expressed in the spinous layer, but not in the basal layer, of the psoriatic lesional epidermis (Fig. 2B and C).

Considerable evidence currently exists to support the concept that psoriasis is mediated by many inflammatory cytokines. There is a predominance of Th1 cytokines, mainly interferon gamma (IFN-γ), in contrast to the predominance of Th2 cytokines found in atopic dermatitis. This immune-mediated aspect of psoriasis pathogenesis has been confirmed by the use of cyclosporine or targeted therapies against T cells, CD11a, or TNF-α [1]. With regard to keratinocytes, psoriatic plaques represent a hyperproliferative condition and deregulated differentiation [1]. Keratinocytes are the main component cells of the epidermis, and the important mechanism for keratinocyte growth is the EGF receptor-ligand system. In this EGF receptor-ligand system, the signal from ErbB1 (EGFR) is important for keratinocyte growth. TGF-α, HB-EGF, amphiregulin and epiregulin are autocrine growth factors and all bind to ErbB1 [2]. Previous reports have shown that TGF-α and amphiregulin mRNA are over-expressed in psoriatic lesional skin and play important roles for the keratinocyte proliferation of psoriatic epidermis, suggesting that all members of the EGF family are up-regulated in psoriatic epidermis [3–5]. In this study, we investigated the mRNA expression of epiregulin as well as TGF-α and amphiregulin in psoriatic and normal epidermis. The mRNA expression of TGF-α and amphiregulin was elevated in psoriatic epidermis, as compared to normal skin, as previously reported. The mRNA expression of epiregulin was also increased in psoriatic epidermis. Over-expressed epiregulin mRNA was localized in the spinous layer, but not in the basal layer, of the psoriatic epidermis. TGF-α and amphiregulin mRNA localization in psoriatic epidermis is within the spinous layer. This deregulated growth factor signaling may contribute to the hyperproliferative condition of psoriasis. In fact, a transgenic mouse with the amphiregulin gene revealed a psoriasis-like phenotype [8]. Based on our results and previous reports, a cross-induction mechanism of the keratinocyte-derived EGF family is involved in the development of psoriatic hyperproliferative epidermis.

Intracellular signaling systems such as Erk/JNK or MAP kinase, which are activated by the EGF family, are up-regulated in psoriatic epidermis [9]. Recent studies have shown that transgenic mice over-expressing a constitutive active form of STAT3 develop a psoriasis-like phenotype [10]. Because these molecules are downstream of EGFR signaling, an over-expressed EGF family may contribute to the pathogenesis of psoriasis by activating signal transduction molecules. Because topical treatment will probably remain the mainstay of psoriasis therapy for most patients, and aberrant expression of epiregulin as well as TGF-α and amphiregulin could facilitate the development of proliferative pathological conditions of psoriasis, additional targeting of such signal transduction molecule and/or growth factors may enhance anti-psoriatic therapy.

In conclusion, we have demonstrated the over-expression of epiregulin in psoriatic epidermis. Autocrine EGF-related growth factors may play an important role in the pathogenesis of psoriasis.

Acknowledgments

This work was partly supported by Health Sciences Research Grants for Research on Specific Diseases from the Ministry of Health, Labor, and Welfare of Japan and a Grant-in-Aid for Scientific Research from the Ministry of Education, Culture, Sports, Science, and Technology of Japan. We would also like to thank Teruko Tsuda and Eriko Tan for their technical assistance.

References

[1] Schon MP, Boehncke WH. Psoriasis. N Engl J Med 2005;352:1899–912.
[2] Hashimoto K. Regulation of keratinocyte function by growth factors. J Dermatol Sci 2000;24:S46–50.
[3] Cook PW, Pittelkow MR, Keeble WW, Graves-Deal R, Coffey Jr RJ, Shipley GD. Amphiregulin messenger RNA is elevated

in psoriatic epidermis and gastrointestinal carcinomas. Cancer Res 1992;52:3224–7.
[4] Elder JT, Fisher GJ, Lindquist PB, Bennett GL, Pittelkow MR, Coffey Jr RJ, et al. Overexpression of transforming growth factor alpha in psoriatic epidermis. Science 1989;243:811–4.
[5] Stoll SW, Elder JT. Retinoid regulation of heparin-binding EGF-like growth factor gene expression in human keratinocytes and skin. Exp Dermatol 1998;7:391–7.
[6] Shirakata Y, Komurasaki T, Toyoda H, Hanakawa Y, Yamasaki K, Tokumaru S, et al. Epiregulin, a novel member of the epidermal growth factor family, is an autocrine growth factor in normal human keratinocytes. J Biol Chem 2000;275:5748–53.
[7] Nitta H, Kishimoto J, Grogan TM. Application of automated mRNA in situ hybridization for formalin-fixed, paraffin-embedded mouse skin sections: effects of heat and enzyme pretreatment on mRNA signal detection. Appl Immunohistochem Mol Morphol 2003;11: 183–7.
[8] Cook PW, Piepkorn M, Clegg CH, Plowman GD, DeMay JM, Brown JR, et al. Transgenic expression of the human amphiregulin gene induces a psoriasis-like phenotype. J Clin Invest 1997;100:2286–94.
[9] Zhang X, Yang D, Ma S, Liu H. Up-regulation of activities of mitogen-activated protein kinase in psoriatic lesions. J Dermatol Sci 2005;37:118–9.
[10] Sano S, Chan KS, Carbajal S, Clifford J, Peavey M, Kiguchi K, et al. Stat3 links activated keratinocytes and immunocytes required for development of psoriasis in a novel transgenic mouse model. Nat Med 2005;11: 43–9.

Yuji Shirakata*
Department of Dermatology, Ehime University School of Medicine, Shitsukawa, Toon, Ehime 791-0295, Japan

Jiro Kishimoto
Shiseido Research Center, Tsuzuki-ku, Yokohama, Kanagawa, Japan

Sho Tokumaru
Kenshi Yamasaki
Yasushi Hanakawa
Mikiko Tohyama
Koji Sayama
Koji Hashimoto
Department of Dermatology, Ehime University School of Medicine, Shitsukawa, Toon, Ehime 791-0295, Japan

*Corresponding author.
Tel.: +81 89 960 5350;
fax: +81 89 960 5352
E-mail address: shirakat@m.ehime-u.ac.jp
(Y. Shirakata)

19 April 2006

Cell Tissue Res (2006) 326: 69–77
DOI 10.1007/s00441-006-0208-2

REGULAR ARTICLE

Lujun Yang · Yuji Shirakata · Masachika Shudou · Xiuju Dai · Sho Tokumaru · Satoshi Hirakawa · Koji Sayama · Junji Hamuro · Koji Hashimoto

New skin-equivalent model from de-epithelialized amnion membrane

Received: 14 December 2005 / Accepted: 23 March 2006 / Published online: 7 June 2006

Abstract The presence of pre-existing basement membrane (BM) components improves the morphogenesis of epidermis and BM in constructing a human living skin-equivalent (LSE). De-epithelialized amniotic membrane (AM) retains key BM components. We have therefore investigated the usefulness of AM for constructing LSE. De-epithelialized AM was overlaid on type I collagen gel embedded with fibroblasts. Normal human keratinocytes (NHKs) were then seeded onto the epithelial side of the AM to construct an AM-LSE. A conventional LSE was constructed by seeding NHKs on a fibroblast-populated type I collagen gel. When the keratinocytes reached confluence, the LSE was lifted to the air-liquid interface and cultured for up to 3 weeks. Samples were harvested at various times and investigated morphologically, immunohistochemically, and ultrastructurally. In AM-LSE, the epidermis was better stratified, with more compact, polarized, columnar basal cells, and the expression of differentiation and proliferation markers was more similar to that of normal human skin than was that of LSE without AM. A more continuous BM and better-developed hemidesmosomes were found in AM-LSE. The epidermis of AM-LSE outgrew much faster than that of LSE without AM. When transplanted onto nude mice, both LSEs took well; however, the AM-LSE graft showed better morphogenesis of the epidermis, BM, and hemidesmosomes. The better epidermal morphology and better-developed BM in AM-LSE in vitro and in vivo indicates its superiority over LSE without AM for clinical applications.

Keywords Amniotic membrane · Basement membrane · Keratinocyte · Migration · Skin-equivalent · Human · Mouse (BALB/cAJc1-nu)

This work was partly supported by Health Sciences Research Grants for Research on Specific Diseases from the Ministry of Health, Labor, and Welfare of Japan (to K.H.) and a Grant-in-Aid for Scientific Research from the Ministry of Education, Culture, Sports, Science, and Technology of Japan (to K.H. and Y.S.).
L. Yang and Y. Shirakata contributed equally to this work.

L. Yang · Y. Shirakata (✉) · X. Dai · S. Tokumaru · S. Hirakawa · K. Sayama · K. Hashimoto
Department of Dermatology,
Ehime University School of Medicine,
Shitsukawa,
Toon, Ehime 791-0295, Japan
e-mail: shirakat@m.ehime-u.ac.jp
Tel.: +81-89-9605350
Fax: +81-89-9605352

M. Shudou
Department of Bioscience, Ehime University,
Shitsukawa,
Toon, Ehime 791-0295, Japan

J. Hamuro
ArBlast,
Chuo-ku, Kobe 650-0047, Japan

Introduction

Living skin-equivalent (LSE), which consists of epidermis and dermis matrix, has long been used as a skin substitute for wound closure (Eaglstein and Falanga 1998). A well-developed differentiated epidermis provides a barrier against bacteria and other environmental factors, and the presence of a basement membrane (BM) and fibroblasts are necessary for maintaining epidermal architecture and sustaining growth (Andriani et al. 2003). A variety of biomaterials has been used to construct the dermal matrix of LSE (Guerret et al. 2003; Llames et al. 2004; Meana et al. 1998; Medalie et al. 1997; Ojeh et al. 2001), including type I collagen gel, fibrin gel, human plasma, and acellular human dermis. This shows that BM is not just an inert matrix that supports the epidermis, but that it also regulates epidermal morphogenesis and homeostasis via dynamic cross-talk with the overlying epidermis. Among dermal materials, acellular human dermis possesses an intact BM and supports the epidermis with good morphogenesis and a rete ridge-like pattern. The presence of pre-existing BM component proteins of the dermal matrix is essential for the development of the BM in an LSE (Ralston et al. 1999).

However, large amounts of human dermis are difficult to obtain for clinical application.

Amniotic membrane (AM) is composed of a single layer of columnar epithelial cells, a BM, an acellular compact layer, and the underlying fibroblast and spongy layers (von Versen-Hoynck et al. 2004). The BM zone underlying the amniotic epithelium resembles that of skin morphologically and ultrastructurally and consists of laminin 5 and types IV, VII, and XVII collagen (Oyama et al. 2003). As a biomaterial, AM is readily available and inexpensive and has been used to cover wounds temporarily, thereby reducing inflammation, facilitating epithelialization, and preventing scarring (Sheridan and Moreno 2001; Tseng 2001). De-epithelialized amnion has been employed as a carrier tissue for corneal or oral epithelial cell cultures to make a cornea-equivalent for ocular surface reconstruction (Nakamura et al. 2003a,b, 2004).

Since AM retains the major BM components, AM might be useful for constructing a better LSE. In this study, we have prepared de-epithelialized AM that retains the major BM components and have investigated whether AM improves the epidermis in an LSE. We have seeded keratinocytes onto AMs previously placed (epithelial side up) onto fibroblast-populated type I collagen gels, in order to construct an AM-LSE. Conventional LSEs have also been constructed from the same keratinocytes and fibroblasts by using the same protocol, except for the use of AM. We have further investigated the usefulness of AM for LSE in vitro and in vivo.

Materials and methods

Cell culture

Normal human epidermal keratinocytes (NHKs) were isolated from healthy human skin and cultured under serum-free conditions, as described previously (Shirakata et al. 2003, 2004). The cells were used for LSE cultures in their fourth passage. Fibroblasts were isolated from normal human skin and cultured in DMEM supplemented with 10% fetal calf serum (FCS), and 5th passage cells were used to construct the LSE. All procedures that involved human subjects received prior approval from the Ethics Committee of Ehime University School of Medicine, Toon, Ehime, Japan, and all subjects provided written informed consent.

Preparation of cultured skin-equivalents

The preparation of LSE has been described previously (Yang et al. 2005). Briefly, a collagen gel was prepared by mixing six volumes of ice-cold porcine collagen type I solution (Nitta Gelatin, Osaka, Japan) with one volume of 8×DMEM (Gibco), ten volumes of 1×DMEM supplemented with 20% FCS, and one volume of 0.1 N NaOH. Of this solution, 1 ml was added to each culture insert (Transwel-COL, membrane pore-size: 3 μm, Costar) in a 6-well culture plate (Costar). Following polymerization of the gel in the inserts at 37°C, two volumes of fibroblast suspension solution (5×10^5 cells/ml in 1×DMEM supplemented with 10% FCS) were added to eight volumes of the collagen solution (the final collagen concentration was 0.8 mg/ml), and then 3.5 ml of the fibroblast-containing collagen solution was applied to each insert. When the fibroblast-containing gel polymerized, DMEM supplemented with 10% FCS and ascorbic acid (final concentration: 50 ng/ml) was added. The gel was kept in submerged culture for 5 days, until the fibroblasts contracted the gel.

Human AM was obtained at cesarean section. Under sterile conditions, the AM was washed with sterile phosphate-buffered saline (PBS) and stored at −80°C in 12% dimethylsufoxide in PBS. Before use, the AM was thawed, washed three times with PBS, and cut into pieces (2.5×2.5 cm). The epithelial cells were removed from the AM by incubation in 0.02% EDTA at 37°C for 2 h and then gentle scraping with a cell scraper under a microscope. The spongy layer was also removed. The complete removal of the epithelial cells was confirmed by using hematoxylin and eosin (HE) staining.

The de-epithelialized AM was put, epithelial side up, onto the contracted gel surface, and a stainless steel ring (interior diameter: 11 mm) was overlaid on it to stabilize it. In the hole of the ring, 4×10^5 keratinocytes in 100 μl MCDB 153 type II were seeded onto the AM. The keratinocytes were maintained, submerged in culture, for 2 days. When the keratinocytes reached confluence, the LSE was lifted to the air-liquid interface and cornification medium (a 1:1 mixture of Ham's F-12 and DMEM supplemented with 2% FCS and other supplements; see Yang et al. 2005) was added. The medium was changed every other day. To construct a conventional LSE, keratinocytes were seeded onto the contracted gel and then submerged and airlifted as described above, except for the use of de-epithelialized AM. The stainless steel rings were used to adjust the seeding cell density. Both types of LSE were harvested 7 and 21 days after airlifting. For HE staining, the LSE was fixed in 20% formalin and embedded in paraffin. For immunohistochemical staining, the LSE was snap-frozen in OCT compound. We performed more than 20 experiments, with similar results being obtained in each (a representative experiment is shown in the figures). In comparative studies, keratinocytes and fibroblasts from the same donor were used.

Histology and immunohistochemical staining

Paraffin-embedded LSE samples were sectioned at 6 μm and stained with HE. For immunohistochemical staining, a Histofine Simple Stain MAX-PO (M) kit (Nichirei, Tokyo, Japan) was used according to the manufacturer's instructions. Frozen sections (7 μm) were first incubated with 0.3% hydrogen peroxide for 30 min to remove endogenous peroxidase activity and then incubated with primary antibodies at appropriate dilutions (Table 1) overnight at 4°C. The sections were incubated with enzyme-conjugated

secondary antibodies for 30 min at room temperature and then with the staining substrate. Images were obtained by using an Olympus AX80 microscope coupled with an Olympus DP50 digital camera (Olympus, Tokyo, Japan). We performed at least three independent studies and obtained similar results (a representative experiment is shown in the figures).

Evaluating the epidermal spreading potential of AM-LSEs

Stainless steel rings with an inner diameter of 6 mm were put on gels with or without AM, and 2×10^5 keratinocytes in 30 µl of MCDB 153 II medium were seeded in the hole of each ring. When the keratinocytes reached confluence, the LSEs were lifted to the air-liquid surface, and the stainless steel rings were removed. At days 0, 3, 5, 7, and 10 after being airlifted, epidermal size was measured by using a computer-assisted morphometric analysis. The epidermal size of the conventional and AM-LSEs was compared statistically by using Student's *t*-test.

Transplanting cultured LSEs

The animal grafting protocol was approved by the Ethics Committee of Ehime University School of Medicine. Eight-week-old female BALB/cAJc1-nu nude mice were anesthetized by intraperitoneal injection of 0.3 ml of Avertin (1.25% tribromoethanol, 2.5% 2-methyl-2-butanol solution). Full-thickness wounds were created on the skin of the backs of each mouse by using an 8-mm skin biopsy punch. A piece of AM-LSE or conventional LSE of matching size (7 days after airlift) obtained using the same punch was grafted onto the wound and covered with a transparent film. At 14 days after transplantation, the grafts were harvested. One part of each graft was paraffin-embedded and sectioned at 6 µm. Some sections were stained with HE, and some were de-paraffinized and blocked for endogenous peroxidase activity and then blood vessels were stained with rabbit antibody against type IV collagen (at dilution 1:50; American Research Products, Belmont, Mass.) according to the protocol of the Histofine SAB-AP (R) kit (Nichirei, Tokyo, Japan). Finally, the sections were counterstained with hematoxylin for cell nuclei. One part of each graft was also processed for electron-microscopic analysis. We performed at least three independent studies and obtained similar results (a representative experiment is shown in the figures).

Transmission electron microscopy

Specimens were fixed with 0.1% tannic acid, 2.5% glutaraldehyde in 0.1 M phosphate buffer (pH 7.4) for 2 h, washed with phosphate buffer, postfixed with 1% osmium tetroxide in phosphate buffer for 2 h, washed with 0.25 M sucrose solution, dehydrated in a graded series of ethanol, and embedded in an Epon-resin mixture. Ultrathin sections (<60–80 nm) were prepared by using a Leica Ultracut S, double-stained with uranyl acetate and lead citrate, and examined with a transmission electron microscope (JEM-1230, JEOL, Tokyo, Japan) at 80 kV.

Results

AM-LSE has a better-organized and more mature epidermis

Both AM-LSE and the conventional LSE showed differentiated epidermis with a basal layer, suprabasal layer, and stratum corneum at days 7 and 21 after airlifting (Fig. 1). The epidermal stratification was however better organized in the AM-LSE; the basal cells were cuboid, smaller, and more compact, and aligned along the AM with clear demarcation (Fig. 1a,b). In the conventional LSE, the epidermal stratification was not as well organized. The larger round basal cells were sparsely aligned along the dermal-epidermal junction, and the number of basal cells had decreased considerably by day 21 (Fig. 1e,f).

We found keratin 6, a marker of keratinocyte activation, only in hair follicles in normal human skin sections (Fig. 2). In AM-LSE, keratin 6 staining was faint at day 7 and disappeared almost completely in the basal and lower suprabasal layers by day 21 (Fig. 2a,k). In conventional LSE, the epidermis strongly expressed keratin 6 up to

Table 1 Details of primary antibodies used

Antigen	Clone	Dilution of antibody	Antibody source
E-cadherin	HECD-1	1:100	TaKaRa
Desmoglein 1	27B2	1:100	Zymed
Desmoglein 3	5G11	1:100	Zymed
Keratin 10	LHP1	1:100	NeoMarkers
Keratin 6	LHK6B	1:100	NeoMarkers
Integrin β4	3E1	1:100	Chemicon
Integrin α6	6B4	1:100	Chemicon
Collagen VII	LH7:2	1:100	NeoMarkers
Collagen IV	2311C3	1:200	Chemicon
Laminin 5	GB3	1:100	Sera-lab

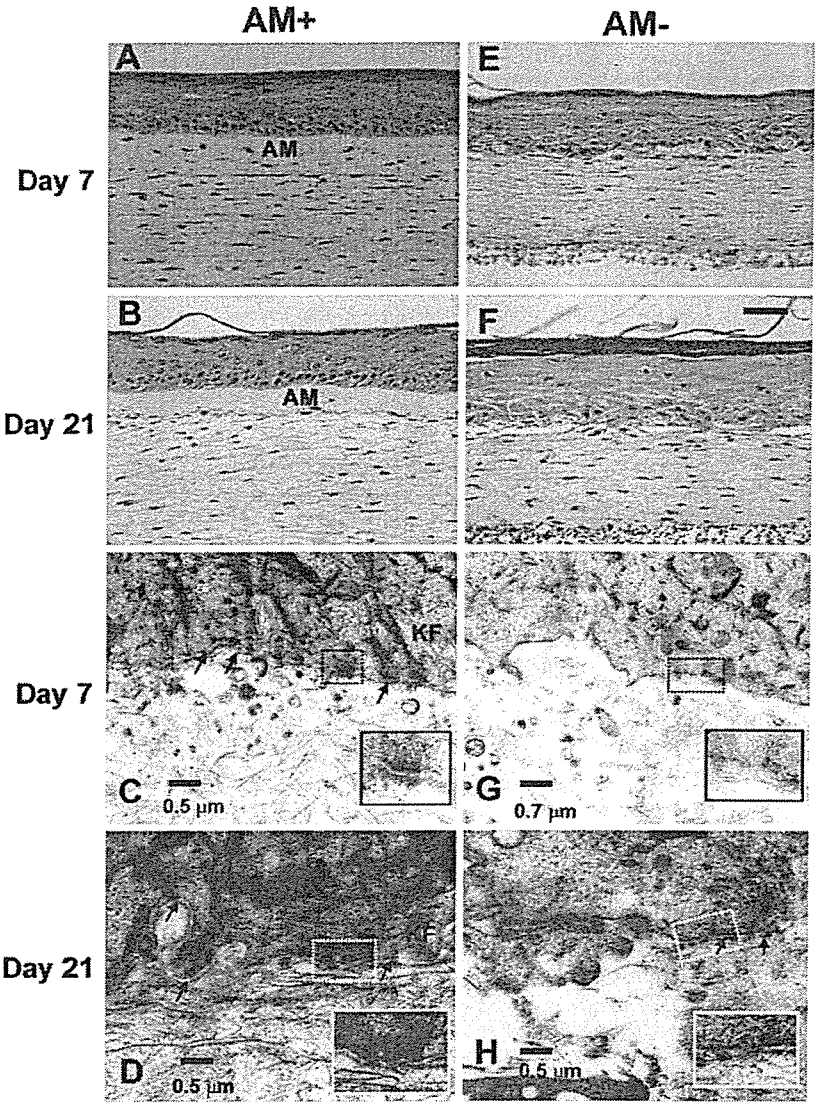

Fig. 1 Morphology of the epidermis and basement membrane (BM) in living skin-equivalent derived from amniotic membrane (AM-LSE; *AM+*) and in conventional LSE (*AM−*). Samples were harvested at days 7 (**a**, **e**, **c**, **g**) and 21 (**b**, **f**, **d**, **h**) from AM-LSE (**a**, **b**, **c**, **d**) and conventional LSE (**e**, **f**, **g**, **h**). Hematoxylin and eosin (HE) staining (**a**, **b**, **e**, **f**) showed a better-stratified epidermis with more compact, columnar basal cells in AM-LSEs. Transmission electron microscopy (**c**, **d**, **g**, **h**) revealed a more continuous lamina densa (*arrows*) and better-developed hemidesmosomes (*insets*) in the AM-LSEs than in the conventional LSEs (*KF* keratin filaments). *Bars* 50 μm (**a**, **b**, **e**, **f**), 0.5 μm (**c**, **d**, **h**), 0.7 μm (**g**)

day 21 after airlifting (Fig. 2f,p). In AM-LSE, keratin 10 expression increased with time, and by day 21, keratin 10 was distributed from the suprabasal layer to the stratum corneum, in a pattern similar to that of normal human skin (Fig. 2b,l). By contrast, keratin 10 expression decreased at day 7 and was barely observed at day 21 in the conventional LSE (Fig. 2g,q). In both LSE models, cell-cell junctions were well developed in similar patterns, as documented by the strongly expressed cell-cell junction proteins, such as E-cadherin (Fig. 2c,h,m,r), desmoglein 1 (Fig. 2d,i,n,s), and desmoglein 3 (Fig. 2e,j,o,t).

Presence of de-epithelialized AM enhances development of BM and hemidesmosomes in LSE

Types IV and VII collagen were present in de-epithelialized AM (data not shown). In the AM-LSE, immunohistochemical staining for types IV and VII collagen was seen along the epidermal-dermal junction at 7 days after airlifting (Fig. 3a,b). The type IV collagen staining was more intense at day 21 (Fig. 3k), whereas less collagen VII was observed (Fig. 3l). In conventional LSE at day 7, only small amounts of collagen IV and VII were noted along the epidermal-dermal junction (Fig. 3f,g), and although the staining increased, it still appeared minimal at day 21 (Fig. 3p,q).

The assembly of the BM was also characterized by determining the distribution of laminin 5 and its receptor, α6β4 integrin. BM normalization could be assessed by the degree to which these proteins were deposited in a polarized linear pattern at the BM zone (Andriani et al. 2003). In AM-LSE, laminin 5 was deposited linearly and was polarized along the epidermal-dermal junction at day 7 (Fig. 3c); the staining intensity had increased by day 21 (Fig. 3m). By contrast, in conventional LSE, little laminin 5 was seen at day 7 (Fig. 3h); by day 21, although more laminin 5 was expressed, its localization was discontinuous and patchy at the suprabasal layer (Fig. 3r). The receptor, α6β4 integrin, was distributed in a pattern similar to that of

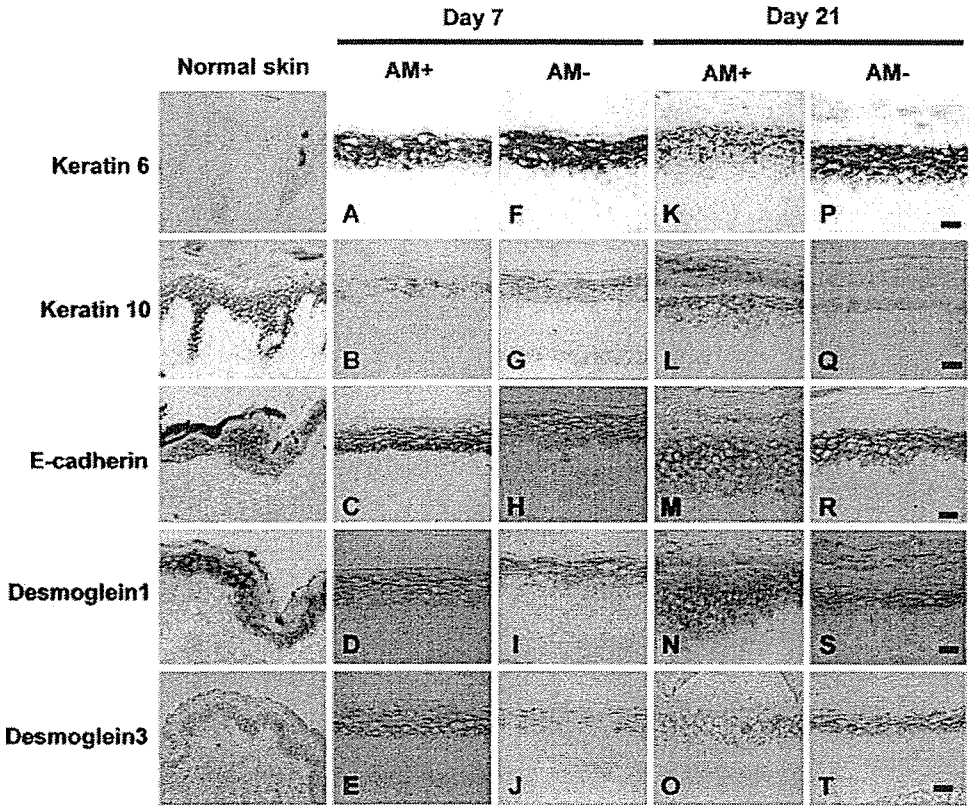

Fig. 2 Keratin and cell-cell junction protein expression in AM-LSE (*AM+*) and conventional LSE (*AM−*). Samples from days 7 (**a-j**) and 21 (**k-t**) from AM-LSEs (**a-e**, **e-o**) and conventional LSEs (**f-j**, **p-t**) were processed for immunohistochemical analysis. The expression of keratin 6 (**a**, **f**, **k**, **p**), keratin 10 (**b**, **g**, **l**, **q**), E-cadherin (**c**, **h**, **m**, **r**), desmoglein 1 (**d**, **i**, **n**, **s**), and desmoglein 3 (**e**, **j**, **o**, **t**) was determined by using the respective monoclonal antibodies. *Bars* 50 μm

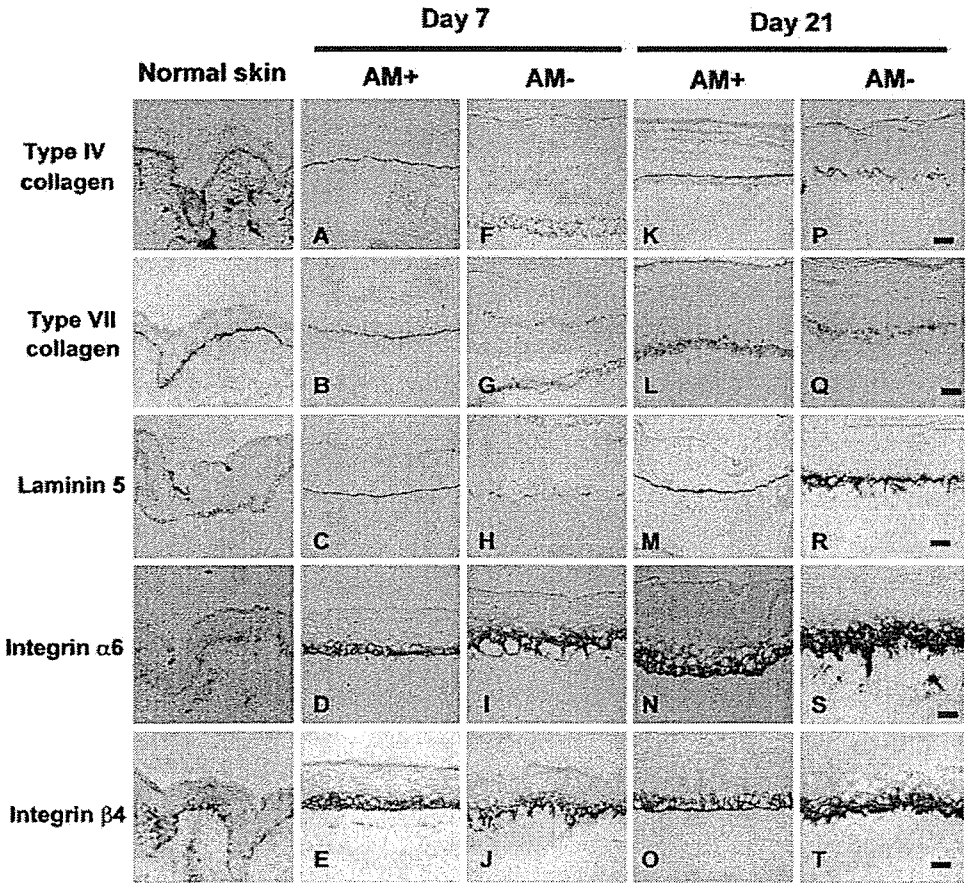

Fig. 3 Integrin and BM component expression in AM-LSE (*AM+*) and conventional LSE (*AM−*). Samples of AM-LSE (**a-e**, **k-o**) and conventional LSE (**f-j**, **p-t**) cultured for 7 (**a-j**) or 21 days (**k-t**) were stained immunohistochemically with monoclonal antibodies against type IV collagen (**a**, **f**, **k**, **p**), type VII collagen (**b**, **g**, **l**, **q**), laminin 5 (**c**, **h**, **m**, **r**), integrin α6 (**d**, **i**, **n**, **s**), and integrin β4 (**e**, **j**, **o**, **t**). *Bars* 50 μm

laminin 5. In AM-LSE, both α6 and β4 integrin subunits were restricted to the basal pole of the basal cells at days 7 and 21 (Fig. 3d,n,e,o). In conventional LSE, α6 and β4 integrin proteins were synthesized and accumulated in the epidermis; they were distributed predominantly in the suprabasal layer and did not localize in a linear pattern (Fig. 3i,s,j,t).

The development of the BM zones of the LSEs was further elucidated by using transmission electron microscopy (TEM) (Fig. 1c,d,g,h). At day 7, a continuous lamina densa was formed along the plasma membrane of the keratinocytes, with many hemidesmosomes, in the AM-LSE. The hemidesmosomes were well developed structurally, with inner and outer plaques clearly being distinguished; keratin filaments were connected to the inner plaques (Fig. 1c), whereas in the conventional LSE, little lamina densa or BM structures were seen at day 7. Along the plasma membrane of the basal cells, some electron-dense hemidesmosome-like structures were seen; however, they did not possess the structural features of hemidesmosomes (Fig. 1g). At day 21, the lamina densa and hemidesmosomes in the AM-LSE were well developed, and the structural features of hemidesmosomes were clearly displayed (Fig. 1d), whereas in conventional LSE, an interrupted lamina densa was seen, with poorly developed hemidesmosomes (Fig. 1h).

De-epithelialized AM improved epidermal outgrowth

On the day of airlifting (day 0), the epidermis of both the AM-LSE and conventional LSE was 6 mm in diameter. The epidermis of the AM-LSE continued to outgrow faster than that of the conventional LSE (Fig. 4): at day 3, the epidermis measured 7.7±0.4 mm (it had increased by 28.3%), and at day 10, it reached 18.3±1.1 mm (over three times its original size). By contrast, the epidermis of the conventional LSE did not change in size by day 3, and only a 78.3% increase to 10.7±0.2 mm was seen at day 10. These results indicated that the AM stimulated keratinocyte migration and proliferation.

AM-LSE grafts on nude mice exhibit better morphogenesis of the epidermis and BM

Two weeks after transplantation, the grafts were harvested and manipulated for observation by light microscopy and TEM. Both the AM-LSE and conventional LSE took well on the recipient nude mice. The fibroblast-populated gel in conventional LSE was prone to separate from the epidermis and was fragile during manipulation. The epidermis of the AM-LSE was tightly attached to the underlying tissue, and the graft was more resistant to rupture. The epidermis of both types of graft was well differentiated with a thick stratum corneum (Fig. 5a,b). The epidermis of the AM-LSE was better stratified than that of the conventional LSE, and the basal cells were columnar and aligned on the surface of the AM (Fig. 5a). By contrast, the epidermal

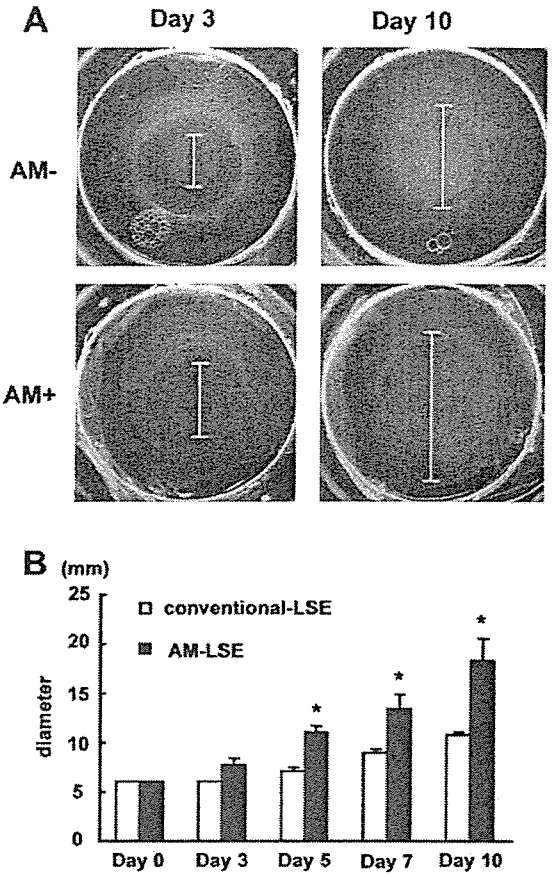

Fig. 4 Comparison of epidermal outgrowth of AM-LSE and conventional LSE. **a** Stainless steel rings with an inner diameter of 6 mm were placed on gels with (*AM+*) or without (*AM−*) AM, and 2×10^5 keratinocytes were seeded. When the keratinocytes reached confluence, the LSEs were lifted to the air-liquid surface, and the stainless steel rings were removed. Epidermal size (*lines*) was monitored after airlifting. **b** The epidermal diameter of AM-LSE and conventional LSE was measured at days 3, 5, 7, and 10, and the mean value for each day was calculated (n=3, $^*P<0.05$)

stratification in the conventional LSE was disorganized, with few basal cells along the dermal-epidermal junction (Fig. 5b).

In the AM- LSE graft, an electron-lucent lamina lucida was clearly observed between the basal cell plasma membrane and the continuous electron-dense lamina densa. Hemidesmosomes were well developed structurally and dotted along the plasma membrane of the basal cells (Fig. 5c). By contrast, the BM in the conventional LSE graft was rudimentary and faint, and far fewer hemidesmosomes were present than in the AM-LSE graft, as seen in vitro (Fig. 5d).

The basal cell number per millimeter in three separate fields of view of both LSE grafts was calculated and showed a significantly higher cell number in AM-LSEs than in conventional LSEs (Fig. 5h). Since vascularization is essential for graft survival, we investigated the angiogenesis in AM-LSE and conventional LSE. We found the AM-LSE grafts were better vascularized, with even some capillaries infiltrating into the AM (Fig. 5e), whereas blood

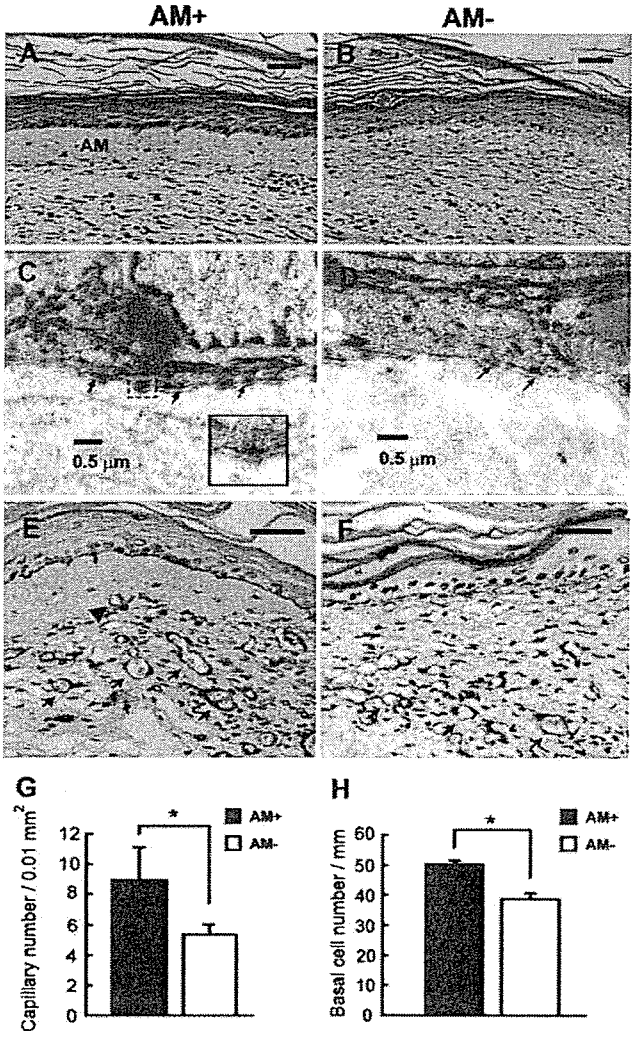

Fig. 5 Light-microscopic and ultrastructural views of AM-LSE (*AM+*) and conventional LSE (*AM−*) in vivo. AM-LSE or conventional LSE was grafted onto the back skin of nude mice. Two weeks after transplantation, samples were harvested and processed for HE staining (**a**, **b**), TEM (**c**, **d**), and immunohistochemical staining for type IV collagen to detect blood vessels (**e**, **f**). HE staining showed better organized epidermis (**a**, **b**) and more basal cells (**h**) in AM-LSE grafts than in conventional LSE grafts. TEM revealed a continuous lamina densa (*arrows* in **c**) with many structurally well-developed hemidesmosomes (*inset* in **c**) in the AM-LSE, and a faint interrupted lamina densa (*arrows* in **d**) with fewer, poorly developed hemidesmosomes in the conventional LSE. More blood vessels (*arrows* in **e**, **f**) were found in AM-LSE grafts than in conventional LSE grafts (**e**, **f**, **g**), with some vessels infiltrating into the AM (*arrowhead* in **e**). $^*P<0.05$ (**g**, **h**). *Bars* 50 μm (**a**, **b**, **e**, **f**), 0.5 μm (**c**, **d**)

vessels were fewer in conventional LSE grafts (Fig. 5f). The number of blood vessels/0.01 mm^2 in three separate fields of view was calculated and revealed significantly more blood vessels in AM-LSE grafts than in conventional LSE (Fig. 5g).

Discussion

Epithelial-mesenchymal interactions play important roles in controlling epidermal morphogenesis and homeostasis. The interaction between keratinocytes and the insoluble BM proteins contributes to the maintenance of tissue architecture and affects various biological processes, such as cell attachment, proliferation, differentiation, and migration (Blomme et al. 1998; Kim et al. 1994). In autologous split-thickness skin grafting for treating deep burns, a disturbance in BM reassembly is believed to be responsible for post-burn blisters (Bergman et al. 1997). In conventional LSEs constructed by seeding keratinocytes on a fibroblast-populated type I collagen gel, the BM is not well developed a few weeks after airlifting and is rarely seen after their transplantation onto nude mice (Amano et al. 2001; Medalie et al. 1997).

During the construction of a LSE, pre-existing BM components on the dermal matrix contribute to improving the morphology of the epidermis and are necessary for the formation of hemidesmosomes and the development of a lamina densa (Kim et al. 2001; Medalie et al. 1997; Ralston et al. 1999). The de-epithelialized AM is immunohistochemically positive for types VII and IV collagen, but negative for laminin 5 (data not shown), which is probably lost during the EDTA treatment and subsequent mechanical scraping used to remove epithelial cells from the AM. In this study, we have constructed LSEs with or without de-epithelialized AM to investigate the usefulness of AM. The same types of keratinocytes and fibroblasts and the same techniques have been used for both types of LSE in order to elucidate the roles of de-epithelialized AM in epidermal morphology, BM development, and epidermal migration. We have compared the two types of LSE morphologically, immunohistochemically, and ultrastructurally.

The results indicate that the presence of certain BM components on de-epithelialized AM improve the epidermogenesis of the overlaying epidermis, which is more mature and better organized than epidermis without AM. Similar effects of BM proteins have also been documented in a composite skin-equivalent by using, as the substrate, acellular dermis, which retains several key BM components (Medalie et al. 1997; Ralston et al. 1999). The sustained growth of the keratinocytes in an LSE is maintained by a well-developed BM (Andriani et al. 2003), whose formation is facilitated by the pre-existing BM components.

Laminin 5 is also essential for epidermal-dermal adhesion. Laminin 5 bridges integrin $\alpha6\beta4$ with underlying connective tissue through an association with laminin 6 and 7 and direct binding to type VII collagen (Champliaud et al. 1996; Rousselle et al. 1997). The effect of pre-existing BM components in normalizing the deposition and polarization of laminin 5 has been documented in the construction of LSE by seeding keratinocytes on de-epithelialized dermis (Andriani et al. 2003, 2004). Moreover, the presence of laminin 5 initiates hemidesmosome formation and accelerates the formation of the lamina densa (Nishiyama et al. 2000; Tsunenaga et al. 1998). The de-epithelialized AM

also enhances the polarized basal distribution of α6β4 integrin along the dermal-epidermal junction, as compared with the more suprabasal, albeit denser, distribution in conventional LSEs.

The well-developed basal lamina and hemidesmosomes and the polarized basal deposition of laminin 5 and α6β4 integrin guarantee a stable association between the epidermis and the underlying tissues in AM-LSEs. This might explain why the epidermis is more resistant to separation from the underlying connective tissue during the manipulation of AM-LSEs, as compared with the loose connection in conventional LSEs.

The outgrowth of corneal explants has been reported to be faster on de-epithelialized AM than on intact AM; this implies that the exposed extracellular matrix of de-epithelialized AM is more inducive to epithelial cell migration (Koizumi et al. 2000). Of the BM components, collagen IV had been shown to assist keratinocyte migration through an interaction with keratinocyte α2β1 integrin (Kim et al. 1994). In AM-LSEs, the epidermis outgrows much faster than when on a fibroblast-populated type I collagen gel; AM-LSEs might thus better meet the clinical need to provide a skin-equivalent for a larger area in a shorter time.

AM-LSE therefore appears superior to conventional LSE in several ways (see above). We have transplanted AM-LSE and conventional LSE onto nude mice and found that both LSEs take well on full-thickness wounds of nude mice. A better-organized epidermis, continuous lamina densa and lamina lucida, better-formed hemidesmosomes, and more importantly, better vascularization are seen with AM-LSE. When manipulating the graft for transplantation, the AM-LSE is much more resistant to rupture, as compared with the fragile conventional LSE.

However, the lack of the BM zone in conventional LSE can be supplemented not only by the epidermal side of the de-epithelialized amnion, but also by the stromal side of the amnion, which can support the growth of fibroblasts (Espana et al. 2003; Kumar et al. 2003). This implies that amnion could provide a scaffold for LSE, greatly simplifying the procedures for making dermal matrix and avoiding the use of animal collagen, which is costly and ethically problematic. Moreover, the limited immunogenicity and immune-privilege of amnion (Kubo et al. 2001; Mahgoub et al. 2004), together with its anti-inflammatory effects (Park and Tseng 2000), make it a suitable material for transplantation and a biological immune barrier for xenotransplantation, which may facilitate allograft transplantation of AM-LSE. Amnion can be readily obtained from cesarean delivery under screening for viral diseases and can also be sterilized and preserved at low cost for long periods without obvious architectural changes (Ravishanker et al. 2003; Rejzek et al. 2001; von Versen-Hoynck et al. 2004), thereby ensuring the plentiful supply of amnion in clinical application. Usually, we can take five to six pieces of amnion of 40–50 mm in size in one delivery. Amnion of this size is easily manipulated, fits the commonly used transwell culture insert (diameter: 75 mm), and can be tailored and used in one piece to cover fresh wounds or made into mesh grafts or stamp grafts to cover granulation tissue as split skin grafts.

In conclusion, the AM-LSE had good epidermal morphology and a well-developed BM zone and is easy to manipulate during transplantation. Since AM is readily obtainable, and since a large amount of AM can be supplied compared with other materials, an AM-LSE should be a good skin substitute for treating burns, ulcers, and other skin defects.

Acknowledgements We thank Teruko Tsuda, Eriko Tan, and Wakana Itoh for technical assistance.

References

Amano S, Akutsu N, Matsunaga Y, Nishiyama T, Champliaud MF, Burgeson RE, Adachi E (2001) Importance of balance between extracellular matrix synthesis and degradation in basement membrane formation. Exp Cell Res 271:249–262

Andriani F, Margulis A, Lin N, Griffey S, Garlick JA (2003) Analysis of microenvironmental factors contributing to basement membrane assembly and normalized epidermal phenotype. J Invest Dermatol 120:923–931

Andriani F, Garfield J, Fusenig NE, Garlick JA (2004) Basement membrane proteins promote progression of intraepithelial neoplasia in 3-dimensional models of human stratified epithelium. Int J Cancer 108:348–357

Bergman R, David R, Ramon Y, Ramon M, Kerner H, Kilim S, Peled I, Friedman-Birnbaum R (1997) Delayed postburn blisters: an immunohistochemical and ultrastructural study. J Cutan Pathol 24:429–433

Blomme EA, Weckmann MT, Capen CC, Rosol TJ (1998) Influence of extracellular matrix macromolecules on normal human keratinocyte phenotype and parathyroid hormone-related protein secretion and expression in vitro. Exp Cell Res 238: 204–215

Champliaud MF, Lunstrum GP, Rousselle P, Nishiyama T, Keene DR, Burgeson RE (1996) Human amnion contains a novel laminin variant, laminin 7, which like laminin 6, covalently associates with laminin 5 to promote stable epithelial-stromal attachment. J Cell Biol 132:1189–1198

Eaglstein WH, Falanga V (1998) Tissue engineering and the development of Apligraf a human skin equivalent. Adv Wound Care 11:1–8

Espana EM, He H, Kawakita T, Di Pascuale MA, Raju VK, Liu CY, Tseng SC (2003) Human keratocytes cultured on amniotic membrane stroma preserve morphology and express keratocan. Invest Ophthalmol Vis Sci 44:5136–5141

Guerret S, Govignon E, Hartmann DJ, Ronfard V (2003) Long-term remodeling of a bilayered living human skin equivalent (Apligraf) grafted onto nude mice: immunolocalization of human cells and characterization of extracellular matrix. Wound Repair Regen 11:35–45

Kim JP, Chen JD, Wilke MS, Schall TJ, Woodley DT (1994) Human keratinocyte migration on type IV collagen. Roles of heparin-binding site and alpha 2 beta 1 integrin. Lab Invest 71:401–408

Kim SW, Park KC, Kim HJ, Cho KH, Chung JH, Kim KH, Eun HC, Lee JS, Park KD (2001) Effects of collagen IV and laminin on the reconstruction of human oral mucosa. J Biomed Mater Res 58:108–112

Koizumi N, Fullwood NJ, Bairaktaris G, Inatomi T, Kinoshita S, Quantock AJ (2000) Cultivation of corneal epithelial cells on intact and denuded human amniotic membrane. Invest Ophthalmol Vis Sci 41:2506–2513

Kubo M, Sonoda Y, Muramatsu R, Usui M (2001) Immunogenicity of human amniotic membrane in experimental xenotransplantation. Invest Ophthalmol Vis Sci 42:1539–1546

Kumar TR, Shanmugasundaram N, Babu M (2003) Biocompatible collagen scaffolds from a human amniotic membrane: physicochemical and in vitro culture characteristics. J Biomater Sci Polym Ed 14:689–706

Llames SG, Del Rio M, Larcher F, Garcia E, Garcia M, Escamez MJ, Jorcano JL, Holguin P, Meana A (2004) Human plasma as a dermal scaffold for the generation of a completely autologous bioengineered skin. Transplantation 77:350–355

Mahgoub MA, Ammar A, Fayez M, Edris A, Hazem A, Akl M, Hammam O (2004) Neovascularization of the amniotic membrane as a biological immune barrier. Transplant Proc 36: 1194–1198

Meana A, Iglesias J, Del Rio M, Larcher F, Madrigal B, Fresno MF, Martin C, San Roman F, Tevar F (1998) Large surface of cultured human epithelium obtained on a dermal matrix based on live fibroblast-containing fibrin gels. Burns 24:621–630

Medalie DA, Eming SA, Collins ME, Tompkins RG, Yarmush ML, Morgan JR (1997) Differences in dermal analogs influence subsequent pigmentation, epidermal differentiation, basement membrane, and rete ridge formation of transplanted composite skin grafts. Transplantation 64:454–465

Nakamura T, Endo K, Cooper LJ, Fullwood NJ, Tanifuji N, Tsuzuki M, Koizumi N, Inatomi T, Sano Y, Kinoshita S (2003a) The successful culture and autologous transplantation of rabbit oral mucosal epithelial cells on amniotic membrane. Invest Ophthalmol Vis Sci 44:106–116

Nakamura T, Koizumi N, Tsuzuki M, Inoki K, Sano Y, Sotozono C, Kinoshita S (2003b) Successful regrafting of cultivated corneal epithelium using amniotic membrane as a carrier in severe ocular surface disease. Cornea 22:70–71

Nakamura T, Yoshitani M, Rigby H, Fullwood NJ, Ito W, Inatomi T, Sotozono C, Nakamura T, Shimizu Y, Kinoshita S (2004) Sterilized, freeze-dried amniotic membrane: a useful substrate for ocular surface reconstruction. Invest Ophthalmol Vis Sci 45:93–99

Nishiyama T, Amano S, Tsunenaga M, Kadoya K, Takeda A, Adachi E, Burgeson RE (2000) The importance of laminin 5 in the dermal-epidermal basement membrane. J Dermatol Sci 24: S51–S59

Ojeh NO, Frame JD, Navsaria HA (2001) In vitro characterization of an artificial dermal scaffold. Tissue Eng 7:457–472

Oyama N, Bhogal BS, Carrington P, Gratian MJ, Black MM (2003) Human placental amnion is a novel substrate for detecting autoantibodies in autoimmune bullous diseases by immunoblotting. Br J Dermatol 148:939–944

Park WC, Tseng SC (2000) Modulation of acute inflammation and keratocyte death by suturing, blood, and amniotic membrane in PRK. Invest Ophthalmol Vis Sci 41:2906–2914

Ralston DR, Layton C, Dalley AJ, Boyce SG, Freedlander E, MacNeil S (1999) The requirement for basement membrane antigens in the production of human epidermal/dermal composites in vitro. Br J Dermatol 140:605–615

Ravishanker R, Bath AS, Roy R (2003) "Amnion Bank"—the use of long term glycerol preserved amniotic membranes in the management of superficial and superficial partial thickness burns. Burns 29:369–374

Rejzek A, Weyer F, Eichberger R, Gebhart W (2001) Physical changes of amniotic membranes through glycerolization for the use as an epidermal substitute. Light and electron microscopic studies. Cell Tissue Bank 2:95–102

Rousselle P, Keene DR, Ruggiero F, Champliaud MF, Rest M, Burgeson RE (1997) Laminin 5 binds the NC-1 domain of type VII collagen. J Cell Biol 138:719–728

Sheridan RL, Moreno C (2001) Skin substitutes in burns. Burns 27:92

Shirakata Y, Tokumaru S, Yamasaki K, Sayama K, Hashimoto K (2003) So-called biological dressing effects of cultured epidermal sheets are mediated by the production of EGF family, TGF-beta and VEGF. J Dermatol Sci 32:209–215

Shirakata Y, Ueno H, Hanakawa Y, Kameda K, Yamasaki K, Tokumaru S, Yahata Y, Tohyama M, Sayama K, Hashimoto K (2004) TGF-beta is not involved in early phase growth inhibition of keratinocytes by 1alpha,25(OH)2vitamin D3. J Dermatol Sci 36:41–50

Tseng SC (2001) Amniotic membrane transplantation for ocular surface reconstruction. Biosci Rep 21:481–489

Tsunenaga M, Adachi E, Amano S, Burgeson RE, Nishiyama T (1998) Laminin 5 can promote assembly of the lamina densa in the skin equivalent model. Matrix Biol 17:603–613

von Versen-Hoynck F, Syring C, Bachmann S, Moller DE (2004) The influence of different preservation and sterilisation steps on the histological properties of amnion allografts-light and scanning electron microscopic studies. Cell Tissue Bank 5:45–56

Yang L, Shirakata Y, Tamai K, Dai X, Hanakawa Y, Tokumaru S, Yahata Y, Tohyama M, Shiraishi K, Nagai H, Wang X, Murakami S, Sayama K, Kaneda Y, Hashimoto K (2005) Microbubble-enhanced ultrasound for gene transfer into living skin equivalents. J Dermatol Sci 40:105–114

THE JOURNAL OF BIOLOGICAL CHEMISTRY VOL. 281, NO. 31, pp. 22013–22020, August 4, 2006

Transforming Growth Factor-β-activated Kinase 1 Is Essential for Differentiation and the Prevention of Apoptosis in Epidermis*

Received for publication, February 3, 2006, and in revised form, April 17, 2006 Published, JBC Papers in Press, June 5, 2006, DOI 10.1074/jbc.M601065200

Koji Sayama[‡1], Yasushi Hanakawa[‡], Hiroshi Nagai[‡], Yuji Shirakata[‡], Xiuju Dai[‡], Satoshi Hirakawa[‡], Sho Tokumaru[‡], Mikiko Tohyama[‡], Lujun Yang[‡], Shintaro Sato[§], Akira Shizuo[§], and Koji Hashimoto[‡]

From the [‡]Department of Dermatology, Ehime University School of Medicine, Ehime 791-0295 and the [§]Research Institute for Microbial Disease, Osaka University, Suita 565-0871, Japan

Transforming growth factor-β-activated kinase 1 (TAK1) is a member of the mitogen-activated protein (MAP) kinase family and is an upstream signaling molecule of nuclear factor-κB (NF-κB). Given that NF-κB regulates keratinocyte differentiation and apoptosis, TAK1 may be essential for epidermal functions. To test this, we generated keratinocyte-specific TAK1-deficient mice from *Map3k7*$^{flox/flox}$ mice and *K5-Cre* mice. The keratinocyte-specific TAK1-deficient mice were macroscopically indistinguishable from their littermates until postnatal day 2 or 3, when the skin started to roughen and wrinkle. This phenotype progressed, and the mice died by postnatal day 7. Histological analysis showed thickening of the epidermis with foci of keratinocyte apoptosis and intra-epidermal micro-abscesses. Immunohistochemical analysis showed that the suprabasal keratinocytes of the TAK1-deficient epidermis expressed keratin 5 and keratin 14, which are normally confined to the basal layer. The expression of keratin 1, keratin 10, and loricrin, which are markers for the suprabasal and late phase differentiation of the epidermis, was absent from the TAK1-deficient epidermis. Furthermore, the TAK1-deficient epidermis expressed keratin 16 and had an increased number of Ki67-positive cells. These data indicate that TAK1 deficiency in keratinocytes results in abnormal differentiation, increased proliferation, and apoptosis in the epidermis. However, the keratinocytes from the TAK1-deficient epidermis induced keratin 1 in suspension culture, indicating that the TAK1-deficient keratinocytes retain the ability to differentiate. Moreover, the removal of TAK1 from cultured keratinocytes of *Map3k7*$^{flox/flox}$ mice resulted in apoptosis, indicating that TAK1 is essential for preventing apoptosis. In conclusion, TAK1 is essential in the regulation of keratinocyte growth, differentiation, and apoptosis.

The epidermis is a multilayered epithelial tissue, maintained by the precise regulation of keratinocyte proliferation, differentiation, and cell death. Cell growth is limited to the basal cell layer, which attaches to the basement membrane. After leaving the basement membrane, keratinocytes differentiate and form a multilayered epidermis instead of undergoing apoptosis. This keratinocyte differentiation is regulated by intracellular signaling pathways involving nuclear factor-κB (NF-κB),[2] the MAP kinase family, phosphatidylinositol 3-kinase, and protein kinase C (1–3).

In the epidermis, NF-κB is found in the cytoplasm of basal cells (1). The functional blockade of NF-κB by expressing dominant negative NF-κB in transgenic mouse epidermis produced a hyperplastic epithelium *in vivo* (1). With deficiency of the p65/RelA subunit of NF-κB, the epidermis is hyperplastic (4). Conversely, the overexpression of active p50 (a subunit of NF-κB) and p65 in the transgenic epithelium produced hypoplasia and growth inhibition, suggesting a role for NF-κB in negative cellular growth control (1). Furthermore, the expression of active p50 and p65 in keratinocytes inhibits cell cycle progression to G_1 arrest *in vitro*, which was associated with an increased p21 level (5) and CDK4 down-regulation (6). This CDK4 regulation is dependent on both the TNFR1 and JNK pathways (7). In addition to regulating differentiation and cell growth, NF-κB protects keratinocytes from apoptosis, and the blockade of NF-κB function in the epidermis by the expression of the dominant negative mutant IκBα provoked premature spontaneous cell death (8). Although the roles of the NF-κB pathway have been studied in keratinocytes, the upstream signal of the NF-κB pathway has not been clarified fully.

Transforming growth factor-β-activated kinase 1 (TAK1), a member of the MAP kinase kinase kinase family, is a signaling molecule upstream from NF-κB and is encoded by the *Map3k7* gene. TAK1 was originally identified as a signaling molecule activated by transforming growth factor β (9). TAK1 is also involved in IL-1 signaling and TNF-α-induced activation of NF-κB and MAP kinases (MAPKs). Activated TAK1 is recruited to TRAF6 and TRAF2, in response to the IL-1 and TNF receptors, respectively (10–12). TAK1 forms a complex

* This work was supported by grants from the Ministries of Health, Labor, and Welfare and Education, Culture, Sports, Science, and Technology of Japan. The costs of publication of this article were defrayed in part by the payment of page charges. This article must therefore be hereby marked "*advertisement*" in accordance with 18 U.S.C. Section 1734 solely to indicate this fact.

[1] To whom correspondence should be addressed: Dept. of Dermatology, Ehime University School of Medicine, Toon, Ehime, 791-0295, Japan. Tel.: 81-89-960-5350; Fax: 81-89-960-5350; E-mail: sayama@m.ehime-u.ac.jp.

[2] The abbreviations used are: NF-κB, nuclear factor-κB; TAK1, transforming growth factor-β-activated kinase 1; MAP, mitogen-activated protein; MAPK, MAP kinase; IKK, IκB kinase; KO, knock-out; K, keratin; Ax, adenovirus vector; P, postnatal day; TAB, TAK1-binding protein; TEWL, trans-epidermal water loss; TUNEL, TdT-mediated dUTP nick end-labeling; RT, reverse transcriptase; JNK, c-Jun NH_2-terminal kinase; IL, interleukin; TNF, tumor necrosis factor; poly-HEMA, polyhydroxyethylmethacrylate; LDH, lactate dehydrogenase.

with TAK1-binding protein (TAB) 1, TAB2, and TAB3 (10, 12–14). The activated TAK1 complex phosphorylates IκB kinases (IKKs) and MAPK kinase 6, which activate NF-κB and MAPKs, respectively. The transfection of TAK1 small interfering RNA markedly inhibited TNF-α- and IL-1-mediated activation of NF-κB (11). Recently, TAK1 was shown to be essential for innate and adaptive immune responses by generating B cell-specific TAK1 deficiency (15).

Given that TAK1 is an upstream signaling molecule of the NF-κB pathway, TAK1 might regulate keratinocyte growth, differentiation, and apoptosis. However, the function of TAK1 in epidermal keratinocytes has not been studied. To address this issue, we generated keratinocyte-specific TAK1-deficient mice by using Cre-recombinase transgenic mice under the control of the K5 promoter.

EXPERIMENTAL PROCEDURES

Generation of Keratinocyte-specific TAK1-deficient Mice Using Gene Targeting with the Cre Transgene—The targeting construct has been described previously (15). We generated keratinocyte-specific TAK1-deficient mice by breeding *Map3k7*$^{flox/flox}$ mice with mice carrying the *Cre* transgene under the control of the keratin 5 promoter (*K5-Cre*) (16). The *Map3k7*$^{flox/flox}$ mice were bred with *K5-Cre* mice to generate *K5-Cre/Map3k7*$^{flox/+}$ mice. Subsequently, the *K5-Cre/Map3k7*$^{flox/+}$ mice were bred to *Map3k7*$^{flox/flox}$ mice to generate *K5-Cre/Map3k7*$^{flox/flox}$ mice. The genotype of each mouse was confirmed using PCR and Western blot analysis. The TAK1 primer sequences were 5′-GGAACCCGTGGATAAGTG-CACTTGAAT-3′ and 5′-GGCTTTCATTGTGGAGGTA-AGCTGAGA-3′. The amplified products were 320 bp for the floxed allele and 280 bp for the wild-type allele. The Cre-recombinase primers were 5′-TTACCGGTCGATGCAACGAGT-GATG-3′ and 5′-TTCCATGAGTGAACGAACCTGGTCG-3′. Isolated keratinocytes were cultured overnight, and the adherent keratinocytes were harvested for Western blot analysis (see Fig. 1*D*). This protocol was approved by the Institutional Review Board of Ehime University School of Medicine.

Trans-epidermal Water Loss (TEWL)—TEWL was measured using a Tewameter TM210 (Integral Co., Tokyo, Japan) according to the manufacturer's instructions. The data are expressed as the means ± S.E. The statistical significance was determined using the paired Student's *t* test. The differences were considered statistically significant at $p < 0.01$.

Histological Analysis—Mouse skin was fixed in 3.6% formaldehyde, dehydrated, and embedded in paraffin. Four-μm sections were stained with hematoxylin and eosin.

To analyze differentiation markers, keratin (K) 5, K14, K1, K10, and loricrin, the paraffin-embedded sections were deparaffinized, blocked with 10% goat serum, and reacted with the first antibodies overnight at 4 °C. After washing with phosphate-buffered saline, the first antibodies were detected using a peroxidase staining kit (ImmPRESS; Vector Laboratories, Burlingame, CA) and visualized with the chromogen 3-amino-9-ethyl-cabazole according to the manufacturer's instructions. For K16 and Ki67 staining, the deparaffinized sections were boiled in 10 mM citrate buffer, pH 6.0, for 40 min and cooled at room temperature for 20 min for antigen retrieval. Subsequently, K16 and Ki67 were stained following the same procedure as for the differentiation markers.

Confocal Laser Scanning Microscopy—Frozen skin sections (4 μm) were blocked with 10% goat serum and reacted overnight at 4 °C with rabbit anti p50 and p65. After washing with phosphate-buffered saline, the sections were incubated with Alexa Fluor 488-conjugated donkey anti-rabbit IgG for 30 min at room temperature. The stained specimens were observed under a LSM 510 microscope (Carl Zeiss, Jena, Germany). The images were captured using LSM 510 software.

TdT-mediated dUTP Nick End Labeling (TUNEL)—Keratinocyte apoptosis was detected by the TUNEL method using an *in situ* cell death detection kit (Roche Applied Sciences). After being deparaffinized, the sections were treated with 20 μg/ml proteinase K in 10 mM Tris-HCl, pH 7.4, for 15 min at room temperature and labeled according to the manufacturer's instructions. The labeled cells were observed under a fluorescence microscope.

Antibodies—The following antibodies were used: K5, K14, K1, and K10 (rabbit; Covance, Berkeley, CA); K16 (mouse, clone number LL025; Chemicon International, Temecula, CA); loricrin (rabbit; Covance); Ki67 (mouse, clone number MM1, Novo Castra Laboratories, Newcastle, UK); β-actin (mouse, clone number AC-15, Abcam, Cambridge, UK); and p50, p65, and TAK1 (rabbit, Santa Cruz Biotechnology, Santa Cruz, CA).

Keratinocyte Culture—Primary mouse keratinocytes were isolated from newborn mouse skin. The skin samples were cut into 3–5-mm pieces and incubated with 250 units/ml dispase (Godoshusei, Tokyo, Japan) in Dulbecco's modified Eagle's medium overnight at 4 °C. After the epidermis was separated from the dermis, the epidermal sheets were incubated in a 0.25% trypsin solution for 10 min at 37 °C and teased with forceps. The keratinocytes were collected by centrifugation and were cultured further in CnT-02 medium (CellnTec, Bern, Switzerland).

For suspension culture, keratinocytes were plated onto 6-cm polyhydroxyethylmethacrylate (poly-HEMA)-coated plates (3). The poly-HEMA-coated plates were made by adding 4 ml of a solution containing 10 mg/ml poly-HEMA (Sigma-Aldrich) in ethanol to the dish, drying, and repeating once, followed by extensive phosphate-buffered saline washes. After 24 h, the cells were harvested by pipetting.

Western Blotting—Keratinocytes were harvested on ice with lysis buffer containing 1.0% Nonidet P-40, 1% sodium deoxycholate, 0.1% SDS, 150 mM NaCl, 20 mM Tris-HCl, pH 7.5, 1 mM EDTA, and 0.1% protease inhibitor (Sigma-Aldrich). The proteins (20 μg) were separated by 10% SDS-PAGE and transferred to a nitrocellulose membrane. The membrane was blocked with 5% nonfat dry milk in Tris-HCl, pH 7.4, 0.15 M NaCl, and 0.05% Tween 20 and was incubated with the appropriate first antibody. After washing, the membrane was incubated with fluorescein-labeled goat anti-mouse IgG (1:2,500 dilution) for 1 h. The signal was amplified with an anti-fluorescein antibody conjugated with alkaline phosphatase, followed by the fluorescent substrate AttoPhos (Molecular Dynamics, Sunnyvale, CA). The membrane was scanned using FluoroImager (Molecular Dynamics),